International Geology Review

ISSN: (Print) (Online) Journal homepage: https://www.tandfonline.com/loi/tigr20

# Alkalic to tholeiitic magmatism near a mid-ocean ridge: petrogenesis of the KR1 Seamount Trail adjacent to the Australian-Antarctic Ridge

**Sang-Bong Yi, Mi Jung Lee, Sung-Hyun Park, Keisuke Nagao, Seunghee Han, Yun Seok Yang, Hakkyum Choi, Jongmin Baek & Hirochika Sumino**

**To cite this article:** Sang-Bong Yi, Mi Jung Lee, Sung-Hyun Park, Keisuke Nagao, Seunghee Han, Yun Seok Yang, Hakkyum Choi, Jongmin Baek & Hirochika Sumino (2021) Alkalic to tholeiitic magmatism near a mid-ocean ridge: petrogenesis of the KR1 Seamount Trail adjacent to the Australian-Antarctic Ridge, International Geology Review, 63:10, 1215-1235, DOI: 10.1080/00206814.2020.1756002

**To link to this article:** https://doi.org/10.1080/00206814.2020.1756002

INTERNATIONAL GEOLOGY REVIEW
2021, VOL. 63, NO. 10, 1215–1235
https://doi.org/10.1080/00206814.2020.1756002

Taylor & Francis
Taylor & Francis Group

ARTICLE



# Alkalic to tholeiitic magmatism near a mid-ocean ridge: petrogenesis of the KR1 Seamount Trail adjacent to the Australian-Antarctic Ridge

Sang-Bong Yi[a], Mi Jung Lee[a], Sung-Hyun Park[a], Keisuke Nagao[a], Seunghee Han[a], Yun Seok Yang[a], Hakkyum Choi[a], Jongmin Baek[a] and Hirochika Sumino[b]

[a]Division of Polar Earth-System Sciences, Korea Polar Research Institute, Incheon, Republic of Korea; [b]Department of Basic Science, Graduate School of Arts and Sciences, University of Tokyo, Tokyo, Japan

**ABSTRACT**

Coexisting alkalic and tholeiitic basalt lavas has been identified in a seamount chain located near the Australian–Antarctic spreading ridge. The KR1 Seamount Trail (KR1 ST) is a series of volcanic seamounts extending to the southeast in the spreading direction of the Australian–Antarctic Ridge (AAR). We herein report Sr, Nd and Pb isotopic compositions and (U–Th)/He and K–Ar geochronology for dredge samples from the KR1 ST in order to evaluate mantle processes and the role of enriched components for alkalic to tholeiitic magma generation in this region. The KR1 ST is a medium-sized seamount chain that extends for ~60 km, has a maximum height of ~1600 m above the seafloor, and consists of alkaline basalts and tholeiites with formation ages of ~0.4 Ma to ≤1.3 Ma. The isotopic characteristics of the alkaline basalts ($^{206}Pb/^{204}Pb$ = 19.52–19.91; $^{87}Sr/^{86}Sr$ = 0.7030–0.7033; $^{143}Nd/^{144}Nd$ = 0.5128–0.5130) from the KR1 ST reflect a dominant 'PREMA (or FOZO)' mantle component represented by radiogenic Pb and mildly enriched Sr and Nd isotopic compositions. On the other hand, the weak PREMA (FOZO)-affinity ($^{206}Pb/^{204}Pb$ = 18.89–18.93; $^{87}Sr/^{86}Sr$ = 0.7028–0.7029; $^{143}Nd/^{144}Nd$ = ~0.5130; $^{3}He/^{4}He$ = 7.64 ± 0.13 ($R/R_A$)) coupled with their enriched mid-ocean ridge basalt (E-MORB) characteristics of tholeiites from the KR1 ST largely overlap with the KR1 MORB composition. The potential source materials for the alkaline basalts are considered to be ancient, recycled oceanic crust (i.e. eclogite) as well as sub-KR1 depleted MORB mantle (DMM). Whereas the main source materials for the KR1 ST tholeiites are presumed to be the DMM-dominant lithology with minor recycled material. We interpret the KR1 ST as a submarine hotspot chain that was formed by asthenospheric upwelling and spreading processes that delivered fertile blobs of recycled oceanic crust to the sub-KR1 region. The fundamental reason for sub-KR1 upper mantle enrichment might be attributed to a mantle plume event that possibly occurred prior to the formation of the KR1 ST.

**ARTICLE HISTORY**
Received 4 December 2019
Accepted 12 April 2020

**KEYWORDS**
KR1 Seamount Trail; alkaline basalt; tholeiite; PREMA (FOZO); recycled oceanic crust

## 1. Introduction

In ocean environments, alkaline basalts are mostly found in ocean islands (Bonneville *et al*., 2006; Fitton 2007; Niu, 2007; Humphreys and Niu, 2009; White 2010; Garcia 2015), although some alkaline volcanic rocks are reported in island arcs (Kennedy *et al*., 1990; Edwards *et al*., 1994; Sun and Stern, 2001). Alkaline basalts have also been reported in seamounts near mid-ocean ridges (MORs) (Niu and Batiza 1997; Niu *et al*. 2002; Beutel and Anderson 2007; Staudigel and Clague 2010) or intraplate seamounts for which the initial locations are not clear (Vlastelic *et al*., 1998; Janney *et al*., 2000; Bonneville *et al*., 2002; Geldmarcher *et al*., 2005; Hoernle *et al*., 2011a). Accordingly, a number of studies have discussed whether the alkaline magmatism identified in these seamounts is related to the development of MOR, or whether it is the result of deep mantle upwelling (i.e. a mantle plume) to form an ocean island (Niu *et al*. 2002; Beutel and Anderson 2007; Humphreys and Niu, 2009; Hoernle *et al*., 2011b; Brandl *et al*., 2012; Chadwick *et al*., 2014; Long *et al*., 2019). In addition, as mantle plumes have also been reported to be co-located with MORs, and as MOR rift systems can be primarily formed by a mantle plume, compositions of alkaline volcanic rocks found in the ocean environments can be important keys for interpreting the formation processes of MORs as well as seamounts and ocean islands. Oceanic tholeiites are the predominant rocks that form the seafloor and are mainly produced at MORs. However, as these tholeiites are also reported in ocean islands related to mantle plumes (e.g. Hoernle and Schmincke 1993; Albarède *et al*. 1997; Geldmacher *et al*., 2001, 2006; Clague and Sherrod 2014; Poland 2015), the coexistence of alkaline

**CONTACT** Mi Jung Lee mjlee@kopri.re.kr Division of Polar Earth-System Sciences, Korea Polar Research Institute, Songdomirae-ro 26, Yeonsu-gu, Incheon 21990, Republic of Korea
Supplementary data for this article can be accessed here.

basalts and tholeiites near MORs rises the question of whether these rocks are solely related to the MOR or they were produced as a result of deep mantle upwelling unrelated to the MOR.

The Australian–Antarctic Ridge (AAR) corresponds to the eastern end of the Southeast Indian Ridge (SEIR; Figure 1(a)). Park *et al*. (2019) referred to the MOR from east of the Australian–Antarctic Discordance (AAD) to the Macquarie Triple Junction as the AAR, which is adopted in the present study. The AAD has been proposed to be a boundary that defines the components of the Indian and Pacific upper mantle domains (e.g. Christie *et al*. 1998; Kempton *et al*. 2002; Hanan *et al*. 2004). Park *et al*. (2019) collectively named the upper mantle domains including the AAR, which is located east of the AAD, and the far western portion of the Pacific–Antarctic Ridge (PAR) as the Zealandia–Antarctic domain. The Zealandia–Antarctic mantle domain shows distinct Pb and Hf isotope differences between the Indian and Pacific mantle domains, and Park *et al*. (2019) proposed the cause to be a large-scale deep mantle upwelling associated with the Gondwana break-up.

The present study discusses the geochemical nature of the KR1 Seamount Trail (KR1 ST) that is located in the central region of the KR1 ridge segment at the eastern end of the AAR. The KR1 ST is a volcanic seamount chain adjacent to the MOR, the KR1 spreading ridge, which extends parallel to the southeast direction of the KR1 spreading (Yi *et al*. 2019; Figure 1(b)). This study explains the formation of the KR1 ST in conjunction with the development of the KR1 spreading ridge and discusses the formation process of the KR1 ST. Since the KR1 ST

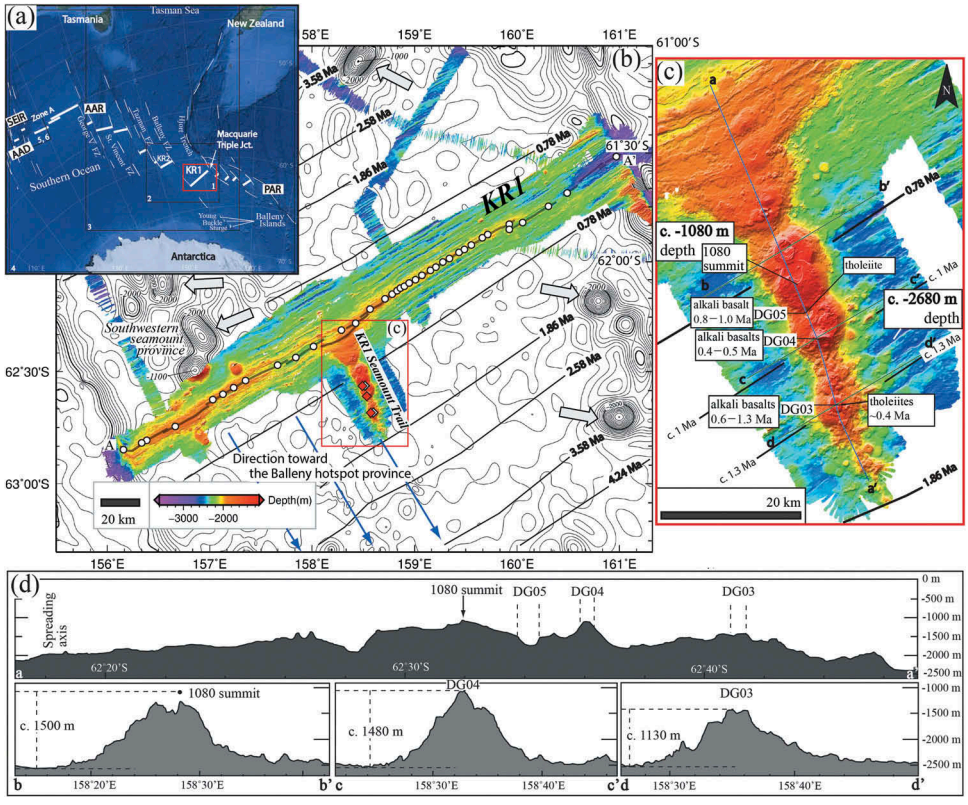


**Figure 1.** (a) The Southern Ocean comprising the Australian–Antarctic Ridge (AAR) and the KR1 segment. Previous researches in and around the AAR: 1, Yi *et al*. (2019); 2, Choi *et al*. (2017); 3, Lanyon *et al*. (1993); 4, Park *et al*. (2019); 5, Hanan *et al*. (2004); 6, Kempton *et al*. (2002). The satellite image is obtained from Google Earth. Bathymetric information is from Christie *et al*. (1999), Cande and Stock (2004) and Choi *et al*. (2017). (b) Bathymetric map of the KR1 study area including sample locations (modified from Yi *et al*. 2019; Park *et al*. 2019) and ocean floor magnetic anomaly ages (after Choi *et al*. 2017). Samples with radiogenic Pb isotopic signature ($^{206}Pb/^{204}Pb$ >19.5, alkaline basalts; this study) are shown as red diamonds, and samples with less radiogenic Pb isotopic signature ($^{206}Pb/^{204}Pb$ <19.2, tholeiites and MORBs) are shown as white diamonds (this study) and circles (Park *et al*. 2019). Stubby arrows on the map indicate seamounts with the height of over 1,000 m. On-axis position lines (A–A′) are presented as a topographic profile in Figure 6a. The Balleny province comprises the Balleny Islands, the Balleny Seamounts and the Anare Seamounts (see bathymetric details: Johnson *et al*. 1982). (c) Enlarged bathymetric map showing the KR1 Seamount Trail (KR1 ST; modified from Yi *et al*. 2019) and dredge sampling locations with concordant/quasi-concordand (U–Th)/He and K–Ar ages of basalt samples. (d) Longitudinal profile (a–a′) and cross section profiles (b–b′, c–c′ and d–d′) of the KR1 ST. Abbreviations: SEIR, Southeast Indian Ridge; AAD, Australian–Antarctic Discordance; PAR, Pacific–Antarctic Ridge; Jct., Junction.

shows morphologies related to hotspot chain and consists of alkaline basalts and tholeiites, this seamount trail might be interpreted as the magmatic result of a mantle plume at first glance. Indeed, the Sr–Nd–Pb isotopic compositions of the KR1 ST basalts presented in this study indicate that these magmas include an enriched mantle component. However, the reported seismic tomography models do not show a deep mantle large buoyancy flux (i.e. mantle plume) beneath the KR1 region (Courtillot *et al*. 2003; Montelli *et al*. 2006; Ritsema *et al*., 2011). Therefore, we will discuss the geochemical properties of the KR1 ST volcanic rocks based on the reported seismic tomography data, as well as the role of deep mantle upwelling, such as mantle plume, in producing mantle heterogeneity beneath the KR1 region.

## 2. Geological setting and topography of the KR1 ST

The KR1 study area is the spreading segment at the southeast end of the AAR. The KR1 ridge segment connects the PAR and the Hjort Trench at the Macquarie Triple Junction (Figure 1(a)). In the KR1 segment, there are a number of medium-size seamounts of >1000 m in height, and the KR1 ST as well as a group of seamounts (Southwestern seamount province) with a height of > 1500 m is developed around the spreading axis. The KR1 spreading ridge (MOR) develops axial plateaus in two zones, and the KR1 ST and Southwestern seamount province develop off-axis in these areas (Figure 1(b)). Bathymetric maps generated through using a multibeam echo sounder (Kongsberg EM122) and dredged rock samples were obtained in 2013 through the regular Korea Polar Research Institute (KOPRI) cruise using the R/VIB *Araon*.

The KR1 ST is a submarine volcanic mountain range developed within the KR1 ridge segment, which begins at a location slightly off-axis of the spreading centre and extends in the south-eastward spreading direction. In the longitudinal section of the KR1 ST, the height increases gradually from the spreading centre towards the 1080 summit (1080 mbsl: ~1,500 m above the surrounding seafloor). The height gradually decreases after passing two peaks of the 1080 and DG04 summits, and the KR1 ST dissipates 60 km away from the spreading centre (Figure 1(c, d)). Samples were dredged at three locations (DG05, DG04 and DG03) southeast of the 1080 summit. Yi *et al*. (2019) reported that these areas mainly comprised alkaline basalts and tholeiites, although ice-rafted clasts from Antarctica were recovered with oceanic basalts in the DG05 area (bathymetric depression). Both alkaline basalts and tholeiites were sampled in the DG03 and DG05 areas, whereas only alkaline basalts were found in DG04 area (a second peak of the KR1 ST). The magnetic anomaly age of the seafloor just south of the KR1 ST has been estimated to be 1.86 Ma (Choi *et al*. 2017); hence, the formation age of the KR1 ST is younger than this (Figure 1(b, c)). The KR1 ST develops parallel to the southeast spreading direction of the KR1 ridge segment with a maximum height of >1500 m and ~60 km length. No submarine volcanic ranges similar to the KR1 ST develops in the northwest direction of the KR1 spreading centre; however, the Southwestern seamount province, which consists of ~1500 m height seamounts and is located to the west of the KR1 ST, develops in the northwest off-axis of the KR1 spreading centre. The Balleny province (Balleny hotspot) is located ~450 km away in a south-eastern direction (i.e. the KR1 spreading direction) to Antarctica parallel with the KR1 ST–Southwestern seamount province (Figure 1; Johnson *et al*., 1982).

## 3. Analytical methods

Sr, Nd and Pb isotope analyses were conducted at the KOPRI following the analytical procedures presented in Lee *et al*. (2015) and Kim *et al*. (2019). Selected fresh glassy basalt chips, 1–2 mm in diameter, were leached in 2 N HCl at 70°C for 10 minutes in an ultrasonic bath and washed in Milli-Q® water to remove possible remaining contaminants. The leached materials were ground using an agate mortar. Approximately 30 mg of each powdered sample were dissolved in HF and $HClO_4$ at 120°C for ~3 days. Pb was separated using an anion exchange column (0.5 mL column volume, AG1-X8, 100–200 mesh resin) with a HBr medium and was then collected with 6 N HCl. Pb column chemistry was repeated twice to obtain further purified Pb fractions. After Pb separation, Sr and Nd were purified using 4 mL of AG50 W-X8 (100–200 mesh, Biorad) and 0.7 mL of AG50 W-X8 (200–400 mesh, Biorad) resin, respectively. Nd was separated from the bulk rare earth element (REE) fraction using 0.22 M alpha hydroxyisobuteric acid (α-HIBA) (Shibata and Yoshikawa 2004).

Sr, Nd and Pb isotopic compositions were measured with a thermal ionization mass spectrometer (TIMS; TRITON, Thermo Scientific) equipped with seven faraday cups at KOPRI. Normalization values of $^{86}Sr/^{88}Sr = 0.1194$ and $^{146}Nd/^{144}Nd = 0.7219$ were applied to correct for Sr and Nd isotope fractionation. Replicate measurements of the NBS 987 and JNdi-1 standards yielded $^{87}Sr/^{86}Sr = 0.710264 \pm 0.000002$ (N = 15, 2σ) and $^{143}Nd/^{144}Nd = 0.512113 \pm 0.000002$ (N = 15, 2σ). Pb isotopic ratios were determined by a Pb double-spike technique using the Southampton-Brest-Lead 207–204 (SBL74)

solution. Replicate analyses of the NBS 981 standard yielded means of $^{206}Pb/^{204}Pb$ = 16.940 ± 0.002, $^{207}Pb/^{204}Pb$ = 15.498 ± 0.002 and $^{208}Pb/^{204}Pb$ = 36.720 ± 0.004 (N = 15; 2σ). The blank levels of Sr, Nd and Pb were generally less than 30 pg for Sr, 20 pg for Nd and 50 pg for Pb, which were negligible compared to the abundances in the analysed samples.

He, Ne and Ar isotopic compositions and $^{84}Kr$ and $^{132}Xe$ concentrations were measured using a noble gas mass spectrometric system, modified-VG5400 (MS-IV), at the Department of Basic Science, Graduate School of Arts and Sciences, University of Tokyo (e.g. Sumino *et al*. 2001). Nine basalt whole-rock samples weighing between 179 mg and 400 mg were wrapped with thin Al-foil (10 μm thick) and inserted into a glass sample holder. After connecting the sample holder to a noble gas extraction furnace, the entire noble gas extraction and purification line were baked for around 17 hours to obtain an ultrahigh vacuum condition. During the baking, the sample holder was heated to 150°C to desorb atmospheric noble gas contamination.

Noble gases in each sample were extracted by heating them to 1800°C for 30 minutes in the Mo-crucible that was degassed by heating to 1850–1900°C repeatedly. Extracted gases were then purified by two Ti–Zr getters heated to 800°C. The purified noble gases were split into two fractions of He–Ne and Ar–Kr–Xe by adsorbing Ar, Kr and Xe onto a charcoal trap cooled by liquid $N_2$. Ne in the He–Ne fraction was adsorbed on a sintered stainless-steel trap cryogenically cooled at 15 K, and the He remaining gas phase was then introduced into the mass spectrometer for isotopic and abundance analysis. After the He analysis, Ne was released from the trap at a temperature of 50 K and then measured for isotopic ratios and abundances. For the analysis of heavier noble gases, Ar, Kr and Xe were released from the charcoal trap at c. 200°C, purified again, and subsequently measured for isotopic ratios and abundances of Ar as well as the abundances of $^{84}Kr$ and $^{132}Xe$. Sensitivities and mass discrimination correction factors of the mass spectrometer system were determined by measuring known amounts of atmosphere with the same procedure applied to the samples. The mass discrimination factor for $^{3}He/^{4}He$ was determined by measuring the HESJ (He Standard of Japan) with $^{3}He/^{4}He = (28.88 \pm 0.14) \times 10^{-6}$ (Matsuda *et al*. 2002). Blank levels were $9.4 \times 10^{-10}$ ($^{4}He$), $1.3 \times 10^{-11}$ ($^{20}Ne$), $4.8 \times 10^{-9}$ ($^{40}Ar$), $3.8 \times 10^{-13}$ ($^{84}Kr$) and $1.0 \times 10^{-13}$ ($^{132}Xe$) in the unit of $cm^3$ STP. Experimental uncertainties for the noble gas concentrations were estimated to be ~10% based on the reproducibility of the standard gas measurements and ambiguity in the gas reduction procedure.

Concentrations of $^{4}He$ and $^{36}Ar$ and $^{3}He/^{4}He$ and $^{40}Ar/^{36}Ar$ ratios are presented in Supplementary Table 1. Abundance ratios of $^{3}He$, $^{4}He$, $^{20}Ne$, $^{84}Kr$ and $^{132}Xe$ normalized on $^{36}Ar$ are presented in Supplementary Table 2, along with those for MOR basalts (MORBs) and air dissolved in seawater in Ozima and Podosek (2002). Noble gas elemental compositions in the $^{84}Kr/^{130}Xe$ *versus* $^{20}Ne/^{36}Ar$ ratios (Saito 1978) show that the three tholeiite samples contain MORB-type noble gases (Supplementary Table 2). Contrastingly, the compositions of most alkaline basalts are in the range of noble gases, largely affected by noble gases dissolved in water, indicating that the majority of gases of mantle origin in the alkaline basalts had been lost and replaced with the noble gases dissolved in ambient seawater.

If abundance ratios of $^{3}He$, $^{4}He$, $^{20}Ne$, $^{36}Ar$, $^{84}Kr$ and $^{132}Xe$ are compared with those of seawater and those of chilled margin of MORBs, tholeiite samples show MORB-type He and Ne abundance patterns, although concentrations of He are much lower than the typical abundances of MORBs (Supplementary Table 2). The low concentrations would have been caused by partial loss of mantle-He from the tholeiites during the cooling after eruption into seawater. For alkaline basalts, however, $^{4}He/^{36}Ar$ is higher than $^{3}He/^{36}Ar$ in the relative abundance patterns, suggesting ingrowth of radiogenic $^{4}He$ from U and Th in the samples. This is also supported by the low $^{3}He/^{4}He$ ratios (0.008–0.93) $\times 10^{-6}$ for the alkaline basalts (Supplementary Table 1).

Loss of He might have occurred during the laboratory work such as preheating to 150°C in a vacuum. Jambon and Shelby (1980) gave He diffusion coefficient ($D_{250}$) of $10^{-8}$ $cm^2/s$ at 250°C and activation energy for diffusion of 14 ± 2 kcal/mole for basaltic glass, which give a diffusion coefficient at 150°C ($D_{150}$) as $4 \times 10^{-10}$ $cm^2/s$ and a diffusion length of 0.007 cm for 17 hours. Hence, the diffusion length of ≤0.1 mm under the preheating condition of 150°C for 17 hours may not cause a serious diffusion loss of He from the samples. However, if the diffusion coefficient becomes larger (e.g. $1 \times 10^{-7}$ $cm^2/s$), the diffusion length increases up to 1 mm, compared to the dimension of the samples, and the (U–Th)/He ages obtained from the samples could be younger than the real ages.

(U–Th)/He and K–Ar ages were calculated through the following procedures, and the results are presented in Supplementary Table 1. The nonlinear Equation (1) was solved by a pinching method approximation to calculate the (U–Th)/He age considering relatively long half-lives of $^{234}U$ ($T_{1/2} = 2.46 \times 10^5$ yr) and $^{231}Pa$ ($T_{1/2} = 3.28 \times 10^4$ yr) in the decay chains of $^{238}U$ and $^{235}U$, respectively:

$$[^{4}He] = 8[^{238}U](e^{\lambda_{238} t} - 1) - 7\lambda_{238}/(\lambda_{234} - \lambda_{238})[^{238}U](1 - e^{(\lambda_{238} - \lambda_{234})t}) + 7[^{235}U](e^{\lambda_{235} t} - 1) - 6\lambda_{235}/(\lambda_{231} - \lambda_{235})[^{235}U](1 - e^{(\lambda_{235} - \lambda_{231})t}) + 6[^{232}Th](e^{\lambda_{232} t} - 1) \quad \text{Eq. (1)}$$

where t, [M] and λ indicate the (U–Th)/He age, isotope concentration and decay constant, respectively.

The measured $^{4}$He is assumed to be *in-situ* produced radiogenic $^{4}$He from U and Th, because $^{3}$He/$^{4}$He ratios are less than $1 \times 10^{-6}$ (Supplementary Table 1). Exceptions are the samples DG05-1 and DG3-4 tholeiites, whose $^{3}$He/$^{4}$He ratios are $10.6 \times 10^{-6}$ and $3.2 \times 10^{-6}$, respectively. For the DG05-1, correction for mantle $^{4}$He was difficult, but for the DG03-4, 30% of total $^{4}$He was subtracted as mantle $^{4}$He. As noted above, He loss might have occurred to some extent from the samples, thus the real (U–Th)/He ages could be older than the calculated ones.

Loss of *in-situ* produced radiogenic $^{40}$Ar may be insignificant compared with He, but excess $^{40}$Ar of mantle origin should be considered, which results in an apparently older K–Ar age than the real one. Identification of the excess $^{40}$Ar, however, is difficult with typical Ar analyses, and another method such as Ar–Ar age dating is required. In the present study, we could apply the K–Ar dating to our samples, and the ages calculated in the following manner should be an upper limit if loss of radiogenic $^{40}$Ar has not occurred from the samples. The excess $^{40}$Ar could be distinct for the tholeiite samples compared to the alkaline basalts, because the presence of mantle-He in these samples strongly suggests a presence of mantle-derived Ar with high $^{40}$Ar/$^{36}$Ar. The low K concentrations of 0.22–0.32 wt. % for the tholeiite samples are an additional disadvantage for K–Ar dating because the low K concentrations can produce $^{40}$Ar as low as $(0.85–1.25) \times 10^{-8}$ cm$^{3}$STP/g for 1 Ma. Such a small amount of radiogenic $^{40}$Ar is not easy to resolve from the mixture of atmospheric Ar, mantle-derived excess $^{40}$Ar and *in-situ* produced radiogenic $^{40}$Ar. The K–Ar ages given in Supplementary Table 1 were calculated assuming that the excess $^{40}$Ar to the atmospheric $^{40}$Ar/$^{36}$Ar = 296 is *in-situ* produced radiogenic $^{40}$Ar after eruption following the formula in Nagao *et al*. (1996), ignoring mantle-derived excess $^{40}$Ar. Hence, real K–Ar ages should be less than the calculated ones, if the mantle-derived excess $^{40}$Ar contributes to the observed $^{40}$Ar in the samples.

## 4. Whole-rock geochemistry

Alkaline basalts of the KR1 ST are glassy or hypocrystalline in texture with olivine (micro)phenocrysts and some vesicles. Tholeiites of the KR1 ST are hypocrystalline or holocrystalline with either plagioclase and clinopyroxene microphenocrysts or aphyric in texture and mostly do not contain vesicles (Supplementary Figure 1).

Alkaline basalts of the KR1 ST have lower silica content and higher alkali ($Na_2O + K_2O$) content than tholeiites that were recovered with them. These alkaline basalts mostly plotted in trachybasalt and basalt areas of the total alkalis *versus* silica (TAS) classification diagram. The composition of two samples among the alkaline basalts corresponds to basanite. Tholeiites in the KR1 ST are seen in the subalkaline basalt and basaltic andesite areas of the TAS diagram (Supplementary Figure 2). The alkaline basalts of the KR1 ST have REE contents and light REE (LREE) enrichment patterns similar to those of ocean island basalts (OIBs) on a chondrite-normalized REE diagram ($La/Sm_N$ = 2.62–3.88; Yi *et al*. 2019). In the primitive mantle-normalized multi-element variation diagram, the KR1 ST alkaline basalts show an enrichment in large ion lithophile elements (LILE; Rb, Ba and Sr) and high field strength elements (HFSE; Th, U, Nb, Ta, Zr and Ti); in particular, they exhibit a prominent positive peak in Nb and Ta and a pronounced trough in Pb. This pattern is similar to the geochemical characteristics of alkaline basalts found in the Balleny province (Lanyon 1994), an intra-plate province close to Antarctica within the KR1 segment, and in the sub-aerial Rurutu young basalts (Cook–Austral islands in the South Pacific; Chauvel *et al*. 1997) (Figure 2). In contrast, tholeiites of the KR1 ST show a weak enrichment in LREE and LILE in comparison to alkaline basalt on a chondrite-normalized REE diagram (Yi *et al*. 2019). In addition, in the primitive mantle-normalized diagram, the KR1 ST tholeiites exhibit a weaker Nb–Ta peak and a shallower Pb trough and slightly higher heavy REE (HREE) contents than those of the alkaline basalts. The tholeiites in the KR1 ST, therefore, show differences in incompatible trace element contents when compared to those of the alkaline basalts that were found with them, yet the two show marked similarities in Nb–Ta and Pb anomaly patterns on the primitive mantle-normalized multi-element variation diagram (Figure 2).

Differences are also distinct in the compositions of Sr, Nd and Pb isotope ratios between the alkaline basalts and the tholeiites. In the $^{143}$Nd/$^{144}$Nd *versus* $^{87}$Sr/$^{86}$Sr plot, the KR1 ST alkaline basalts show mildly enriched $^{143}$Nd/$^{144}$Nd (0.512846–0.512958) and $^{87}$Sr/$^{86}$Sr (0.703004–0.703257) ratios relative to the SEIR and PAR MORB mantles. Their isotope compositions are similar to those of the Balleny province basalts and the Rurutu young basalts. The KR1 ST tholeiites are characterized by lesser enriched $^{143}$Nd/$^{144}$Nd (0.512980–0.513033) and $^{87}$Sr/$^{86}$Sr (0.702760–0.702856) ratios, more depleted than those of the KR1 ST alkaline basalts, and only slightly enriched with respect to most of the KR1 on-axis basalts (i.e. the KR1 MORB; Figure 3 and Supplementary Table 3). The KR1 ST alkaline basalts exhibit considerably radiogenic $^{206}$Pb/$^{204}$Pb ratios of 19.52–19.91, $^{207}$Pb/$^{204}$Pb ratios of 15.59–15.64 and $^{208}$Pb/$^{204}$Pb ratios of 39.16–39.48, mostly overlapping

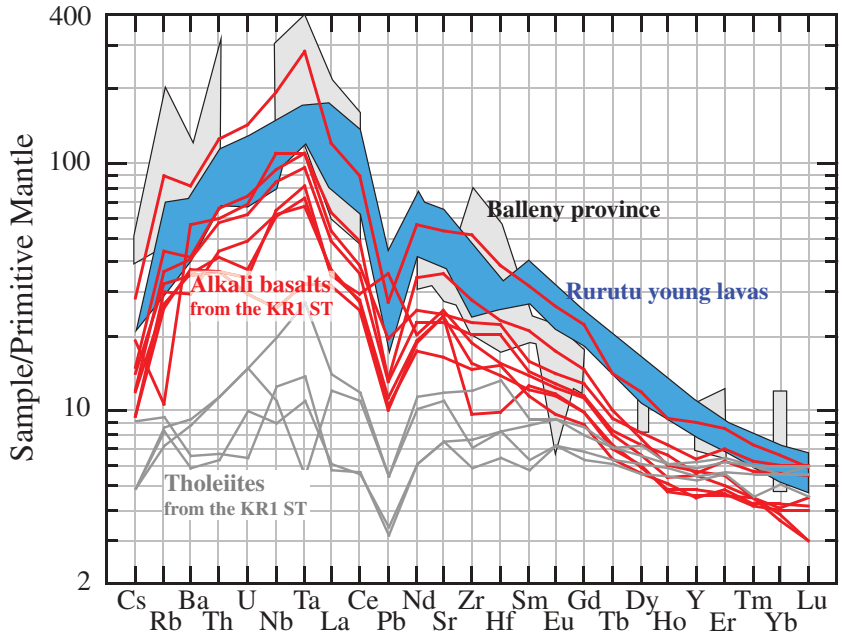


**Figure 2.** Primitive mantle-normalized multi-element variation diagram of basalts from the KR1 ST, seamounts of the Balleny province and young volcanoes on the Rurutu Island. Incompatibility of trace element in this diagram increases from right to left. The geochemical data from the KR1 ST, Balleny province and Rurutu island are from Yi *et al*. (2019), Lanyon (1994) and Chauvel *et al*. (1997), respectively. The primitive mantle composition is from McDonough and Sun (1995).

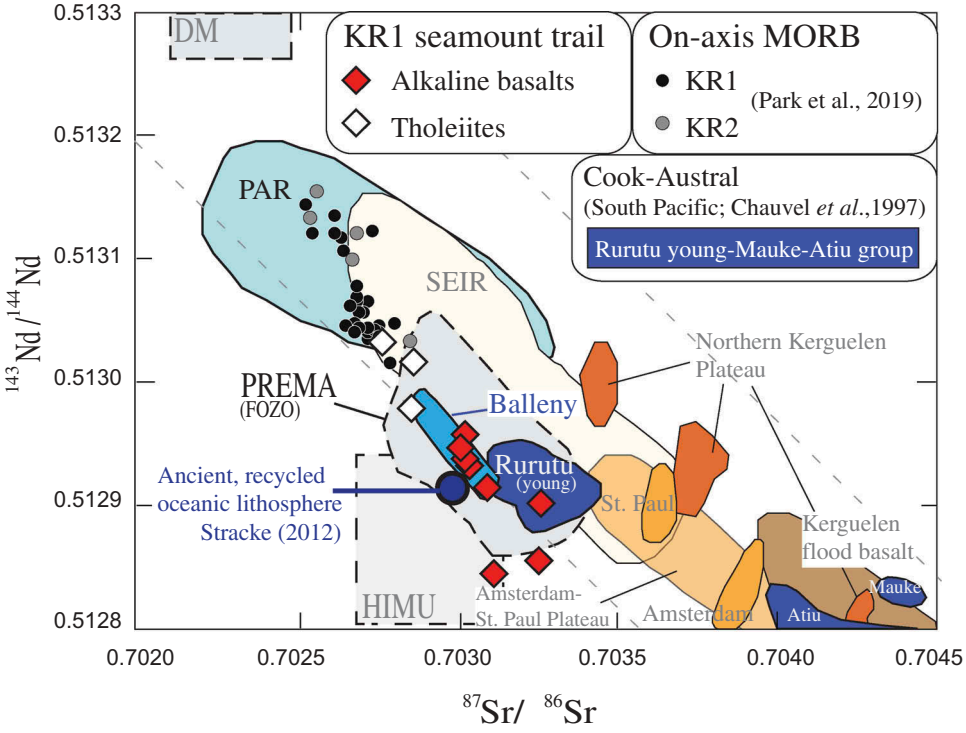


**Figure 3.** Nd and Sr isotopic compositions of the KR1 ST basalts and isotopic comparisons of the KR1 ST basalts with other seamount and ocean island basalts (OIBs), KR1–KR2 on-axis basalts (Park *et al*. 2019) and SEIR (Weis and Frey 2002 and references therein) and PAR (Vlastélic *et al*. 2000) MORBs. Isotope data for OIBs, submarine plateaus and seamounts are from Lanyon (1994), Chauvel *et al*. (1997), Weis *et al*. (2002), Weis and Frey (2002) and references therein. The compositional range of PREMA (FOZO) is taken from Stracke (2012) and Stracke *et al*. (2005). DM and HIMU components are taken from Zindler and Hart (1986).

the Pb–Pb isotope range of the Balleny province basalts. These Pb ratios are slightly less radiogenic than the Rurutu Island basalts (young lava) and are similar to those of the Mauke and Atiu islands within the Cook–Austral chain. The KR1 ST tholeiites have lower radiogenic $^{206}Pb/^{204}Pb$ (18.89–18.93), $^{207}Pb/^{204}Pb$ (15.42–15.54) and $^{208}Pb/^{204}Pb$ (38.47–38.59) ratios in comparison to the KR1 ST alkaline basalts. The KR1 ST tholeiites have Pb isotopic ratios that are similar to those of the KR1 MORB (Figure 4 and Supplementary Table 3).

## 5. Geochronology

(U–Th)/He and K–Ar ages were obtained on alkaline basalts (six samples) and tholeiites (three samples) to investigate the volcanic eruption history of the KR1 ST. The results are presented in Supplementary Table 1.

In the present study, both of the (U–Th)/He and K–Ar ages were calculated using radiogenic components such as $^{4}He$ and $^{40}Ar$ for analysed samples. The (U–Th)/He age generally shows a younger age than the K–Ar age or a similar age. This is thought to be caused by the loss of pre-eruptive $^{4}He$ and/or *in-situ* produced $^{4}He$ from the sample. Additionally, mantle-derived excess $^{40}Ar$ in low-K tholeiites may result in older calculated K–Ar ages as mentioned in Section 3. It is also reported that secular disequilibrium within the (U–Th)/He system may occur in materials with crystallization ages less than c. 1 Ma in relation to chemical fractionation within the $^{238}U$ decay series (Farley *et al.* 2002). Previous studies (e.g. Dalrymple and Moore, 1968; Dalrymple, 1969; Ozima *et al.*, 1977; Seidemann, 1977; Fisher, 1981; Yi *et al.* 2019) suggested that the discordance between (U–Th)/He and K–Ar ages was attributed to age uncertainties for submarine glassy young basalts. Therefore, it is generally considered that a concordant (U–Th)/He and K–Ar age acquired in one sample could be acceptable as an eruption age of the deep-sea basalt (Fisher 1972). Based on these contexts, the present study deals with only the results showing concordant or similar ages between (U–Th)/He and K–Ar ages as possible eruption ages for the KR1 ST basalts.

In the DG03 region, the (U–Th)/He age (0.56 ± 0.05 Ma) and the K–Ar age (1.41 ± 0.15 Ma) of the alkaline basalt (DG03-1) show a slight similarity. Based on about 1.3 Ma of the seafloor age estimated

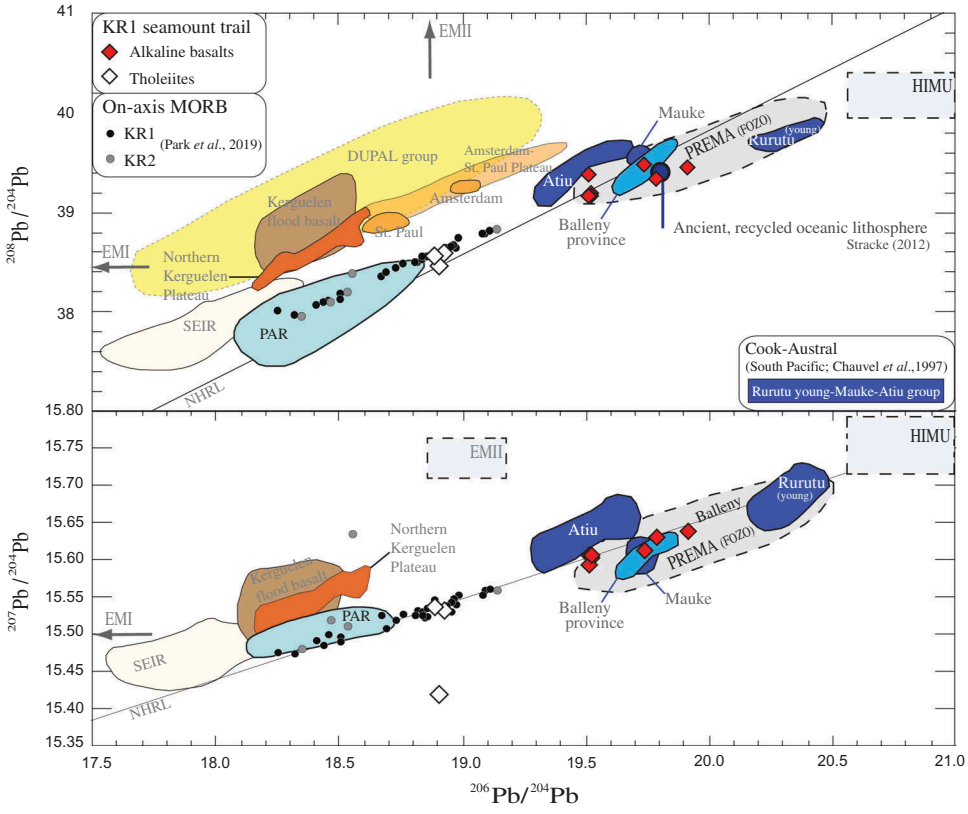


**Figure 4.** Pb isotopic compositions of the KR1 ST basalts and isotopic comparisons of the KR1 ST basalts with other seamount and ocean island basalts, KR1–KR2 on-axis basalts and SEIR and PAR MORBs. Sources of the literature data are the same as in Figure 3. The compositional range of the DUPAL group is taken from Dupré and Allègre (1983). EMI and EMII components are taken from Zindler and Hart (1986), and the Northern Hemisphere reference line (NHRL) is from Hart (1984).

by magnetic anomaly data (Choi *et al*. 2017), the eruption age of alkaline basalt in the DG03 is presumed to be 0.6–1.3 Ma. The (U–Th)/He age (0.40 ± 0.04 Ma) and K–Ar age (0.41 ± 0.07 Ma) of the tholeiite (DG03-2) show a concordant age of c. 0.4 Ma. Thus, tholeiite in the DG03 is considered to have erupted either after or in a similar period to the eruption of alkaline basalt. In the DG04 region, the (U–Th)/He age (0.35 ± 0.03 Ma) and the K–Ar age (0.45 ± 0.20 Ma) of the alkaline basalt (DG04-3) show a concordance, indicating alkaline volcanism occurred at around 0.4–0.5 Ma. In the DG05 region, the (U–Th)/He age (0.75 ± 0.07 Ma) and the K–Ar age (1.30 ± 0.14 Ma) of the alkaline basalt (DG05A) show a slight similarity. As a seafloor age, estimated by magnetic anomaly around the DG04 region, is reported as about 1 Ma (Choi *et al*. 2017), the eruption age of alkaline basalt in the DG05 can be assumed to be 0.8–1.0 Ma (Figure 1(c)). No proper *in-situ* produced radiogenic $^{4}$He concentration for the tholeiite (DG05-1, a thick basalt glass) in the DG05 area was obtained due to the presence of a high concentration of mantle-derived He ($^{3}He/^{4}He = 10.62 \times 10^{-6}$). The $^{3}He/^{4}He$ ratio of the tholeiite DG05-1 (7.64 ± 0.13 ($R/R_A$), where $R_A$ is the atmospheric $^{3}He/^{4}He$ value of $1.39 \times 10^{-6}$) is considered to be a MORB mantle value of the sub-KR1 region.

## 6. Discussion

Oceanic tholeiitic lavas are found in island arcs, MORs and ocean islands. In island arcs, tholeiitic lavas erupt at the beginning of the arc formation, forming a forearc basin or developing into a volcano on the existing oceanic crust (Shervais, 2001; Amma-Miyasaka and Nakagawa, 2002; Dilek and Thy, 2009; Ishizuka *et al*., 2011; Regan *et al*., 2013). The dominant tectonic environment in which oceanic tholeiites can form is a MOR. These tholeiites have varying components from normal-MORB (N-MORB) to enriched-MORB (E-MORB). E-MORB in particular is interpreted to be the result of mantle plume–MOR interaction (Doucet *et al*. 2004; Mertz *et al*. 2004; Dyment *et al*. 2007; Füri *et al*. 2011; Kim *et al*., 2017) or a reflection of the upper mantle heterogeneity derived from the addition of continental and/or oceanic crustal components (Niu and Batiza 1997; Niu *et al*. 2002; Anderson 2006; Beutel and Anderson 2007; Hoernle et al., 2011a; Kim *et al*., 2017). Tholeiites are also observed in ocean islands (ocean island tholeiites, OITs) that are associated with a mantle plume or a prominent mantle upwelling process. These OITs mainly form the basal shield of the island and are usually replaced over time by alkalic lavas (e.g. Hoernle and Schmincke 1993; Albarède *et al*. 1997; Geldmarcher *et al*., 2001, 2006; Clague and Sherrod 2014; Poland 2015).

The tholeiites and alkaline basalts identified in the KR1 ST also have specific meanings. In the given the tectonic environment in which the KR1 ridge segment is located, coexisting tholeiites and alkaline basalts in the KR1 ST cannot be interpreted as a tholeiitic to alkalic transition related to arc formation. However, since the KR1 ST alkaline basalts exhibit whole-rock geochemistries similar to OIBs (Figures 2 and 5(a)) and are enriched in Pb isotopes, this indicates a possibility that the KR1 ST alkaline basalts could have been produced by magmatism related to an ocean island or a hotspot. In addition, as the KR1 ST developed adjacent to a MOR (the KR1 spreading ridge) and the KR1 ST tholeiites and the KR1 MORB both have E-MORB characteristics, both can be discussed in terms of a mantle plume (or medium to small-sized deep mantle upwelling) and mantle heterogeneity characterized by various enrichment components beneath the KR1 segment.

### 6.1. Magma sources of the KR1 ST basalts and KR1 MORBs and formation of the KR1 ST

The KR1 ST developed adjacent to the KR1 axial ridge and parallel to one of the spreading directions of the KR1 segment. This indicates that the formation of the KR1 ST may have been closely related to spreading of the KR1 ridge segment. In addition, given that the tholeiites from the KR1 ST exhibit Sr, Nd and Pb isotopic characteristics similar to those of the KR1 MORB (Figures 3 and 4), it is likely that both rock types originated from a similar source material or that the KR1 ST tholeiites represent MORB that have been migrated due to seafloor spreading. However, we observed that the KR1 ST from the KR1 axial ridge exhibits distinct features from the KR1 spreading ridge; it is quite voluminous to distinguish from the axial ridge, with volcanic additions of up to 1600 m above the surrounding seafloor, and also includes prominent alkaline volcanism. No alkaline basalt has been recovered from the KR1 axial ridge (see Park *et al*. 2019).

The isotopic ratios of the KR1 ST alkaline basalts are characterized by a mild enrichment in $^{143}Nd/^{144}Nd$ and $^{87}Sr/^{86}Sr$ ratios but high $^{206}Pb$ enrichment in the $^{206}Pb/^{204}Pb$ ratio. These features are quite similar to the isotopic characteristics of basalts from the Balleny province (Lanyon *et al*. 1993; Lanyon 1994), which are ~450 km away from the KR1 ST in the spreading direction (Figures 3 and 4). Stracke *et al*. (2005) labelled these radiogenic Pb isotopic characteristics as 'FOZO' (focal zone) but later, Stracke (2012) described them as 'PREMA' (prevalent mantle), which have different isotopic positions from those of Hart *et al*. (1992) and Zindler and Hart (1986), and are ubiquitous in the mantle and provide important signatures in a number of OIB (see

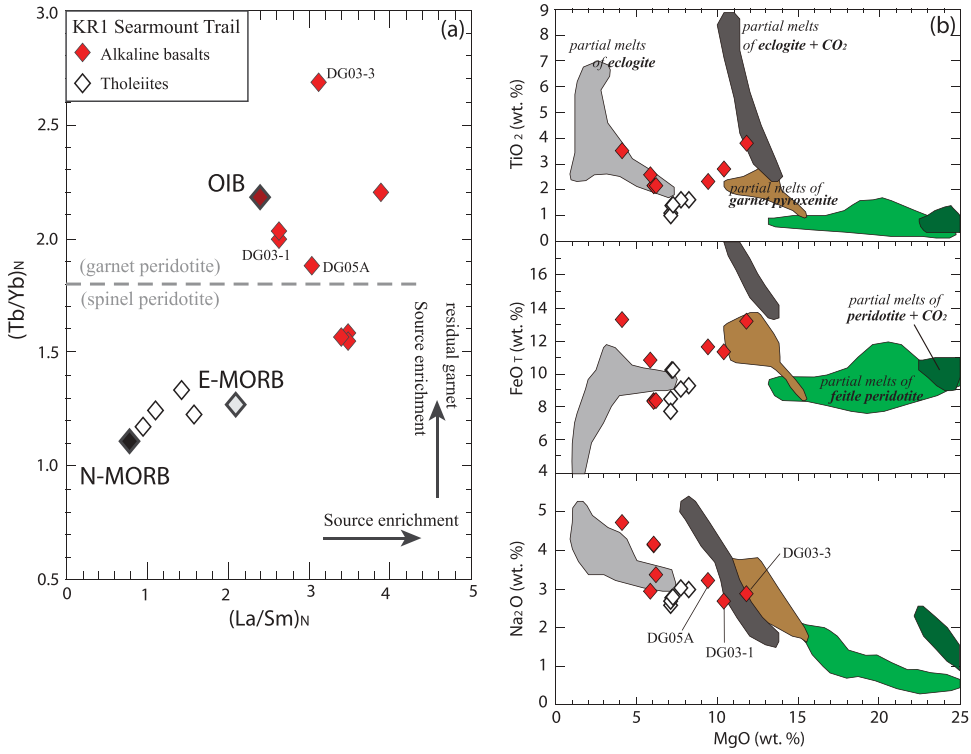


**Figure 5.** (a) The $(La/Sm)_N$ *versus* $(Tb/Yb)_N$ plot. The values were normalized to the primitive mantle (Sun and McDonough, 1989). OIB composition is from Sun and McDonough (1989) and average N- and E-MORB compositions are from Gale *et al.* (2013). A dashed line separating partial melts from spinel and garnet peridotites is taken from Dostal and MacRae (2018). (b) Comparison of the KR1 ST basalt compositions with high-pressure experimental melt compositions of volatile-free fertile peridotite (at 2.5–7.0 GPa; Takahashi, 1986; Hirose and Kushiro, 1993; Walter, 1998; Davies *et al.*, 2011), peridotite + $CO_2$ (at 3.0 GPa; Hirose, 1997), garnet pyroxenite (at 2.0–5.0 GPa; Hirschmann *et al.* 2003; Kogiso *et al.* 2003), eclogite + $CO_2$ (at 3.0 GPa; Dasgupta *et al.* 2006) and volatile-free eclogite (at 2.0-5.0 GPa; Pertermann and Hirschmann, 2003; Spandler et al., 2008). Three primitive alkaline basalts (DG03-1, DG03-3 and DG05) are labelled in the figure.

Stracke *et al.* 2005; Stracke 2012; Jackson *et al.* 2018; Pettke *et al.* 2018). Stracke (2012) pointed out that various isotopic compositions of OIB distributed on the Earth's surface could be explained by the mixing of EM (enriched mantle)–PREMA (or FOZO)–DM (depleted mantle) components. The author suggested that the enrichment of radiogenic Pb, represented by PREMA (FOZO), may have originated from an ancient, recycled oceanic lithosphere that underwent subduction processes. Stracke (2012) also noted that an enrichment in Ta–Nb relative to similarly incompatible trace elements whereas a depletion in Pb relative to Nd in PREMA (FOZO) basalts contrasts with the geochemical characteristics of arc basalts. Hence, the upper oceanic crust is characterized by a relative Ta–Nb enrichment and Pb depletion due to subduction processes (i.e. loss of fluid-mobile trace elements), and the lower oceanic crust undergoes little change in the subduction environment, which could have had radiogenic Pb enriched $^{206}Pb/^{204}Pb$ ratios over a long geological time (e.g. over 2 Ga). The enrichment of radiogenic Pb could be originated by the high U content of seawater and oceanic crust (after seawater interaction) (e.g. Chen *et al.* 1986; Staudigel *et al.* 1995; Niu 2004; Pettke *et al.* 2018); thus basalts, which have the ancient oceanic lithosphere as their main source material, may have the isotopic characteristics of PREMA (FOZO). This signature is quite common in OIB as well as MORB containing PREMA (FOZO)–DM mixing components. This means that the subduction process has been a major geological process in the evolution of the mantle composition and that a large amount of oceanic lithosphere entering the deep mantle over time through subduction processes could inevitably be reflected in the geochemistry of Quaternary basalts.

Alkaline basalt is generally considered to form preferentially under the influence of an alkalinity of source material, high-pressure melting conditions, a low partial melt fraction and $CO_2$-rich volatile involvement (Eggler, 1974; Kinzer and Grove, 1993; Kushiro, 1996, 2001; Finn *et al.*, 2005; Dasgupta *et al.*, 2007). Oceanic alkaline basalts commonly show the enriched radiogenic isotope signatures or the enrichment of incompatible trace elements. These characteristics are believed to have been driven

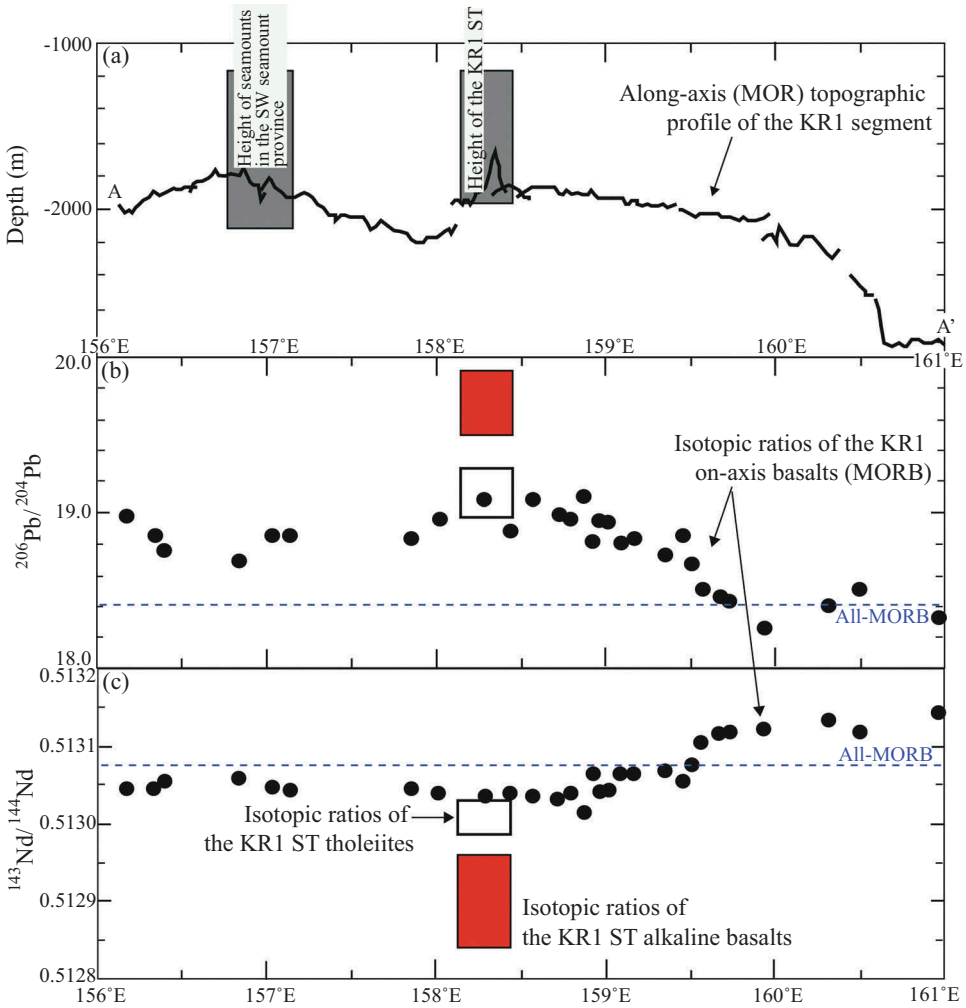


**Figure 6.** Comparison of topographic and isotopic characteristics of the KR1 MOR and KR1 ST: (a) Along-axis (A–A′ lines in Figure 1b) topographic profile of the KR1 MOR (after Park *et al.* 2019) and heights of the KR1 ST and seamounts in the Southwestern seamount province. (b) Compositional variation of $^{206}Pb/^{204}Pb$ and (c) $^{143}Nd/^{144}Nd$ ratios of the KR1 on-axis basalts (MORB; Park *et al.* 2019) with those of the KR1 ST alkaline basalts and tholeiites. All-MORB indicates the mean composition of all possible oceanic ridge segments, including hotspot or mantle plume event areas except back-arc spreading centres (after Gale *et al.* 2013).

mainly by recycled crustal materials within the oceanic upper mantle (Cousens, 1996; Smith, 2005; Sobolev *et al.*, 2007; Willbold and Stracke, 2010; Stracke 2012; Homrighausen *et al.* 2018), or explained as an expression of a primordial mantle signature (Farley *et al.*, 1992; Hilton *et al.*, 1999; Graham, 2002; Hilton and Porcelli, 2003; Hanyu, 2014). These enriched whole-rock isotopic properties and trace element concentrations of the alkaline basalts are considered to be the long-term manifestation of fertile blobs (i.e. recycled crusts) previously enclosed within the lower mantle or to be due to the incorporation of the primordial lower mantle transported via a mantle plume (or deep mantle upwelling). In addition, short-term recycling related to the break-up of a supercontinent or the subduction of oceanic plates is also considered as an important process for producing oceanic alkaline basalts (e.g. Hanan and Graham, 1996; Borisova *et al.*, 2001; Anderson 2006; Hoernle *et al.*, 2011a; Kipf *et al.*, 2014). Previous studies have indicated that off-axis magmatism with a low melt fraction near the MOR could also be associated with the development of alkaline lavas at seamounts (Schouten *et al.*, 1987; Niu and Batiza 1997; Niu *et al.* 2002; Brandl *et al.*, 2012). A ridge–hotspot interaction associated with a mantle plume or the development of a short-lived hotspot has also been suggested as a possible processes to produce alkaline lavas (Fornari *et al.*, 1988; Hoernle *et al.*, 2011b; Chadwick *et al.*, 2014; Long *et al.*, 2019).

The enriched radiogenic Pb concentrations (i.e. the PREMA (FOZO) signature in Stracke 2012) in the KR1 ST alkaline basalts could have originated from the ancient oceanic lithosphere, with the upper ocean crust (i.e. eclo-

gite) appearing to be an important factor in observed isotopic enrichment patterns. Partial melting of eclogite is known to result in a melt with a relatively high content of FeO, $TiO_2$, alkalis and Ni (Hauri 1996). Carbonated eclogite (i.e. $CO_2$ involvement) and garnet pyroxenite (metamorphic deep oceanic crust or metasomatized peridotite) are also considered to produce an alkaline basalt melt (Hirschmann *et al*. 2003; Kogiso *et al*. 2003; Kogiso 2004; Dasgupta *et al*. 2006). Therefore, the recycled oceanic lithosphere (eclogite + garnet pyroxenite + peridotite) or recycled oceanic crust with the upper mantle may be a good candidate for the alkaline basalt source material (e.g. Cordery *et al*. 1997; Kogiso *et al*. 1998, 2003; Dasgupta *et al*. 2006) and could have possibly been a major source of the KR1 ST alkaline basalts. The Nb–Ta enrichment and Pb depletion relative to the similarly incompatible trace elements in the KR1 ST alkaline basalts are interpreted to be the geochemical inheritance from the upper oceanic crust (i.e. eclogite) source that underwent subduction processes. In this study, the source material (i.e. PREMA (FOZO)) for the KR1 ST alkaline basalts is considered to be a combination of depleted MORB mantle (DMM) and subduction-modified ancient oceanic crust.

KR1 ST alkaline basalts and tholeiites exhibit distinct characteristics in incompatible element ratio plot: alkaline basalts show remarkably higher values than tholeiites for $(La/Sm)_N$ and $(Tb/Yb)_N$ ratios (normalized to primitive mantle after Sun and McDonough, 1989; Figure 5(a)). These element ratios have been used to define the source enrichment and source lithology (e.g. Janney *et al*., 2000; Hofmann, 2003; Hoernle *et al*., 2011b; Yi *et al*. 2014, 2019). Distinct incompatible element characteristics between alkaline basalts and tholeiites of the KR1 ST are in good agreement with the Sr–Nd–Pb isotopic ratio distinctions between the two rock types (Figures 3, 4 and 5(a)). The relatively high $(Tb/Yb)_N$ ratios in the alkaline basalts are due to incompatible trace element enrichments and the residual garnet affinities of the source materials. In addition, the KR1 ST tholeiites exhibit E-MORB characteristics (Yi *et al*. 2019) and have enriched Sr–Nd–Pb isotopic ratios relative to those of the PAR basalts, in addition to having higher radiogenic lead isotope concentrations than the SEIR basalts (Figures 3 and 4). This factor suggests that fertile components within the source mantle may have contributed to the formation of tholeiitic magmas in the KR1 ST.

In their major elemental concentrations, the alkaline basalts and tholeiites of the KR1 ST mainly exhibit the mixing components between fertile peridotite partial melts and eclogite partial melts. Particularly, the primitive alkaline basalts (DG03-1, DG03-3 and DG05A) in the KR1 ST are thought to be related to partial melts from carbonated eclogite or garnet pyroxenite partial melts (Figure 5(b)). This suggests that the isotopic and incompatible trace elemental enrichments of the KR1 ST basalts may be attributed to the eclogite (with/without $CO_2$ involvement) fraction within the upper mantle and that upwelling mantle that entrained ocean crustal blobs (i.e. eclogite) could have been their dominant magma source material. Previous studies have suggested that, when the mantle ascends, partial melting of eclogite begins first and this melt can react with the surrounding peridotite to form garnet pyroxenite (e.g. Sobolev *et al*., 2005, 2007; Herzberg, 2006; Mallik and Dasgupta, 2012, 2013, 2014). Several studies have pointed to garnet pyroxenite as a source for basalts in ocean islands (e.g. Hirschmann *et al*. 2003; Keshav *et al*., 2004; Sobolev *et al*., 2005, 2007; Herzberg, 2006). In addition, the similarities between the Sr–Nd–Pb isotopic ratios of the PREMA (FOZO) component represented by 2 Ga oceanic lithosphere proposed by Stracke (2012) and those found in the KR1 ST alkaline basalts indicate that ancient, recycled oceanic crust acts as a key source material in the formation of alkaline basalts, as well as tholeiites, in the KR1 segment (Figures 3 and 4).

The KR1 ST tholeiites have Sr–Nd–Pb isotopic ratios similar to those of the KR1 MORB. In particular, isotopic compositions of the KR1 ST tholeiites overlap those of the enriched KR1 MORBs in Sr–Nd–Pb isotopic plots (Figures 3, 4 and 6). This indicates that the KR1 ST tholeiites and KR1 MORB fundamentally share the same source material. In this case, it remains questionable as to whether the KR1 ST tholeiites are the on-axis MORB that have been migrated due to seafloor spreading, or separate basalts that formed at the axial ridge peripheries. Although the formation age of the KR1 ST tholeiites has not yet been clearly established, the younger concordant (U–Th)/He and K–Ar age of the DG03-2 (c. 0.4 Ma) compared to the age of surrounding seafloor (c. 1.3 Ma, estimated from magnetic anomaly; Choi *et al*. 2017) implies that the DG03 tholeiites are the products of a separate volcanic eruption, which occurred far from the axial ridge, not older axial MORB. The concordant (U–Th)/He and K–Ar ages of alkaline basalts are mostly younger or similar to the surrounding seafloor ages, whereas the (U–Th)/He ages of alkaline basalts are younger than surrounding seafloor. Thus, the KR1 ST basalts are considered to be mostly products of volcanic eruptions occurred either far from the axial ridge or from the axial ridge peripheries, not from on-axis (Figure 1(c) and Supplementary Table 1).

The KR1 ST alkaline basalts have PREMA (FOZO) characteristics in Sr–Nd–Pb isotopic ratios, whereas the KR1 ST tholeiite and KR1 MORBs show the mixing of PREMA (FOZO) and sub-PAR mantle components (Figures 3 and 4). This suggests that the KR1 ST alkaline basalts may contain the

components from the upper mantle (peridotite) + a large contribution of ancient, recycled oceanic crust (eclogite) as its source materials, whereas the KR1 ST tholeiites and the KR1 MORB could have an upper mantle-dominated (i.e. peridotite >> eclogite) lithology as their source material. We infer that more mantle melting occurs beneath the KR1 spreading ridge than beneath the KR1 ST region, which is characteristic of on-axis MOR processes. Along the KR1 segment, an intermediate, full spreading rate of 63–66 mm/yr has been determined (Choi *et al*. 2017); thus, the region beneath the KR1 spreading ridge corresponds to a region where a prominent mantle melting could occur. In this regard, the KR1 ST alkaline basalts could have been produced by a small amount of partial melting whereby the eclogite partial melts affected the distinct geochemistry of the primitive alkaline melts in the KR1 ST. In contrast, along the KR1 spreading ridge, a relatively large amount of partial melting occurred, which diluted the eclogite partial melts with the dominant peridotite partial melts. In the KR1 ST, whole-rock chemical and isotopic differences between the alkaline basalts and the tholeiites can also be attributed to the melt productivity of the mantle. In other words, if the volume of the tholeiite is large and forms a shield in the KR1 ST and alkaline basalts are found in limited locations at the tops of the seamounts, the difference between these two rock types could be attributed to the differences in melt productivity in the mantle (distinctive or dilute eclogite partial melts). However, the spatial distribution of tholeiites and alkaline basalts along the KR1 ST has not yet been confirmed. Alternatively, it is possible to speculate that the supply of eclogite as a magmatic source material was not constant over time during mantle upwelling associated with the formation of the KR1 ST (Figure 7(a)). If there was a period characterized by high eclogite content (e.g. ancient, recycled ocean crust) supplied via the mantle upwelling, there would also be a period of mantle upwelling characterized by a low eclogite content with a predominantly peridotite matrix. The compositionally heterogeneous mantle upwelling and changes in eclogite content over time are also a feasible scenario that can explain the differences between the alkalic and tholeiitic magmas assuming similar melt productivity rates over time beneath the KR1 ST.

### 6.2. Petrogenesis of the KR1 ST and its association with a mantle plume

A volcanic hotspot is a volcanic region or the underlying mantle region that has a low seismic velocity compared to the ambient mantle and usually forms a linear volcanic chain. It has been suggested that volcanic hotspot could form by various mechanisms in addition to the mantle plume theory presented by Morgan (1971) (Morgan 1978; Sleep 1990, 2002; Anderson 1998, 2000; Clouard and Bonneville 2001; Hirano *et al*. 2006; McNutt 2006; Koppers 2011). For example, supplementary to the Morgan-style deep-plume (primary) hotspot, Courtillot *et al*. (2003) proposed secondary hotspots that originate in the mantle transition zone at a depth of 660 km and tertiary hotspots that originate at a shallower depth.

Given the geologic features of asymmetric linear volcanic edifices (extension into the southeast spreading direction) and the scale of the submarine volcanic chain (maximum 1600 m height and ~60 km in length), the

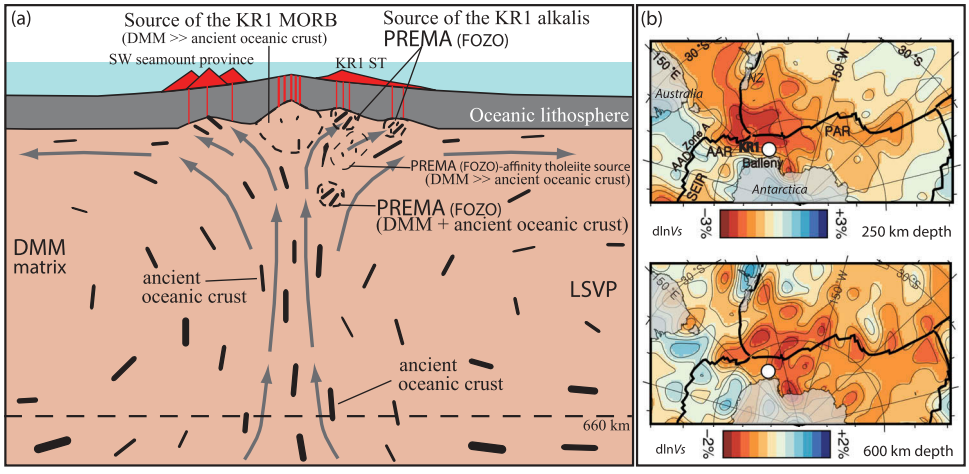


**Figure 7.** (a) Schematic models illustrating formation process of the KR1 ridge segment, including the KR1 ST and the Southwestern (SW) seamount province: The upper mantle beneath the KR1 segment is characterized by a low seismic velocity province (LSVP) containing recycled, ancient oceanic crust (i.e. eclogite). An off-axis magmatism related KR1 axial ridge formation builds the KR1 ST and the SW seamount province. Partial melting process of various proportions of eclogite within the KR1 DMM matrix could make alkalic (PREMA (FOZO)) to tholeiitc (E-MORB composition) basalt magmas. (b) Map of shear-wave velocity variations in the Southern Ocean (after Park *et al*. 2019). Tomographic models of S40RTS (Ritsema *et al*. 2011) at depth of 250 km and 600 km are compared.

KR1 ST could be interpreted as a chain of hotspot volcanoes close to the MOR rather than an extension of the MOR. However, because a deep mantle plume (large buoyancy flux) has not been confirmed in the study area, the KR1 ST cannot be considered as a Morgan-style deep-plume hotspot. Courtillot *et al*. (2003) classified their secondary hotspots to be the result of small- to medium-sized mantle upwelling that diverged from a lower mantle superswell (e.g. South Pacific and African superswells). The tertiary hotspot was classified as a passive response to forms of lithospheric break-up. This tertiary hotspot corresponds to a non-plume hotspot that developed near a MOR as proposed in several previous studies (e.g. Niu and Batiza 1997; Niu *et al*. 2002; Anderson 2006; Beutel and Anderson 2007; Ballmer *et al*., 2013), and is similar to the geologic features of the KR1 ST.

The shear wave velocity ($V_s$) structure of the KR1 segment and its adjacent regions, including the KR1 ST and KR1 spreading ridge, was described by Park *et al*. (2019) as a part of a regional tomographic map that covers the entire Southern Ocean. This tomographic model shows a low seismic velocity province (LSVP) connecting the KR1 ST–southern Hjort trench–westernmost PAR–Balleny province at a 250 km depth (Figure 7(b)). This LSVP extends to a depth of 600 km and part of the LSV region connecting the KR1 ST–Balleny province disappears at a 800 km depth (Courtillot *et al*. 2003; Ritsema *et al*. 2011; Park *et al*. 2019). Therefore, the KR1 ST cannot be regarded as volcanoes formed by a large buoyancy flux ascending from the lowermost mantle, but can be presumed to be a hotspot chain formed during upper mantle upwelling and spreading processes, and could contain the composition of the region beneath the KR1 LSVP (Figure 7(a)).

For the along-axis bathymetric profile of KR1 MOR, the terrain height increases from the northeast segment end to the area adjacent to the KR1 ST (Figure 6(a)). This elevation of topographic height presents patterns similar to the Pb and Nd–Sr–Hf isotope enrichments towards the KR1 ST adjacent area. Moreover, the height of the KR1 on-axis topography increases again towards near the Southwestern seamount province where c. 1500 m seamounts are developed, and the isotopic enrichments were also identified in this on-axis area (Figure 6(b, c) and Park *et al*. 2019). This pattern seems to indicate that the increased mantle upwelling flux that entrains fertile materials (e.g. subducted ancient oceanic crust) may occur beneath the KR1 ST and surrounding on-axis regions and that this mantle upwelling dominates in the regions that include the KR1 ST and the Southwestern seamount province (Figure 7(a)). The source material of the KR1 MORB tholeiites and the KR1 ST tholeiites is considered to be a DMM that contains a small amount of ancient oceanic crust. Seamounts in the Southwestern seamount province require further study from the same point of view as addressed here. These topographic and isotopic features of the KR1 ST and adjacent on-axis regions suggest the possibility of a ridge–hotspot interaction (e.g. Doucet *et al*. 2004; Mertz *et al*. 2004; Dyment *et al*. 2007; Füri *et al*. 2011; Figure 6(a)) as well as off-axis magmatism (e.g. Anderson 2000, 2006; Niu *et al*. 2002; Beutel and Anderson 2007; Ballmer *et al*., 2013) near the MOR where enriched mantle upwelling occurs (Figure 7(a)).

If the PREMA (FOZO) signature identified in the KR1 ST alkaline basalt is an expression of DMM with recycled ancient oceanic crust that was previously subducted, as proposed in Section 6.1, this would require a deep mantle upwelling process (i.e. mantle plume) to form the KR1 upper mantle that encloses fertile oceanic crust pieces prior to the formation of the KR1 ST. A number of studies have discussed that longstanding subduction in Earth's history has given rise to the accumulation of the oceanic lithosphere at the core–mantle boundary, whereby old oceanic crust has been brought to shallow depths by mantle plume (e.g. Silver *et al*. 1988; Davies 1990; Albarède and van der Hilst 1999; Kellogg *et al*. 1999; Homrighausen *et al*. 2018). This mantle plume could be a recent geologic phenomenon or a past phenomenon whose thermal signature has gradually dissipated over time. The presence of both alkaline PREMA (FOZO) basalts and PREMA (FOZO)-affinity tholeiites in the KR1 ST, as well as the presence of PREMA (FOZO)-affinity MORB along the KR1 spreading ridge suggests that the mantle plume event, regardless of when it occurred, could have been involved in producing the PREMA (FOZO) signature in the KR1 region. Although the KR1 ST basalts could reflect the upper mantle characteristics of the KR1 region, the enrichments in incompatible trace elements and radiogenic isotopes in the KR1 ST basalts could have been originally associated with a possible mantle plume event that might occur in the past.

### 6.3. KR1 ST and the Balleny province: a relationship with the South Pacific region

The Balleny Islands (Young, Buckle and Sturge Islands and a number of smaller islands and reefs) are located approximately 450 km southeast (i.e. in the spreading direction of the KR1 segment) from the KR1 ST–Southwestern seamount province. The islands extend for ~180 km in the southeast direction from Young Island. To the northwest of Young Island, the Balleny Seamounts (Slave, Soucek and Ellsworth Banks) developed, which are 350 km from the KR1 ST–Southwestern seamount province in the SE direction. The Anare

Seamounts developed in a northwest–southeast direction adjacent to the Balleny Islands (~70 km northeast of Buckle and Sturge Islands). The Balleny Islands and the adjacent northwest–southeast seamount traces are referred to as the Balleny province in this study (Figure 1(a, b); see bathymetric details in Johnson *et al*. 1982). The orientations of the islands and seamounts in the Balleny province, and the spreading direction of the KR1 ridge segment within the AAR, are closely related. The Sr–Nd–Pb isotopic signatures of the Balleny province volcanoes are also similar to those of the KR1 ST alkaline basalts (Figures 3 and 4). Thus, it is appropriate to discuss the petrogenetic relationship between the KR1 ST and the Balleny province.

Limited studies have reported on the Balleny province due to the difficulty of accessing the region (Johnson *et al*. 1982; Embleton, 1984; Jenkins *et al*., 1992; Lanyon *et al*., 1993; Lanyon 1994). In particular, the results of Sr–Nd–Pb isotope study have been limited to dredge samples from the submarine bank around Buckle Island and the deep seabed between Buckle Island and the Anare Seamounts (Lanyon 1994). Nonetheless, the isotopic signatures of the alkaline basalts (including basanites and a phonotephrite) recovered in these regions are also found in the alkaline basalts from the KR1 ST, which is located ~520 km from the Buckle–Anare region. Age dating results from the Balleny province or major Balleny islands are also insufficient. Although a K–Ar age of 1.76 ± 0.2 Ma has been reported from the Sturge Island volcanic rock (Jenkins *et al*., 1992), it is difficult to constrain the age of the Balleny province volcanoes and the current location of the Balleny hotspot from only one radiometric age measurement. Seafloor magnetic lineations have been used to propose a maximum age of 10 Ma for the onset of the Balleny Islands volcanism (Wright and Kyle, 1990; Green, 1992). Based on the close relationship between the KR1 spreading direction and an elongation of the KR1 ST to the Balleny province, as well as the similar isotopic properties of the KR1 ST–Balleny alkaline basalts, the possibility that the Balleny province could be a chain of seamounts and ocean islands formed near the KR1 spreading ridge cannot be ruled out.

Shear-wave velocity ($V_s$) structure models suggest the possibility that the KR1 ST and the Balleny province could be situated on similar upper mantle types (Figure 7(b); Park *et al*. 2019). This speculation is also consistent with the similar isotopic properties of rocks from the two regions. Lanyon *et al*. (1993) proposed a current mantle plume exist beneath the Balleny Islands, but the global seismic tomography model does not show a LSV zone in the lowermost mantle beneath the region (see Courtillot *et al*. 2003; Montelli *et al*. 2006; Ritsema *et al*. 2011). Therefore, it is unreasonable to interpret volcanic activity in the Balleny province as a direct product of a mantle plume. Additionally, volcanoes in the KR1 ST and surrounding areas are also not direct results of a mantle plume. The isotopic similarities between the alkaline basalts in the KR1 ST and in the Balleny province should instead be explained by the compositional similarities shared by the upper mantles in these two regions. Age dating of the Balleny province basalts should also test the possibility that these regions could be special types of alkaline basalts produced near the MOR (i.e. the KR1 spreading ridge).

The LSVP located 250 km beneath the KR1–Balleny region extends to the PAR, the southern Hjort trench, the Tasman Sea and the Ross Sea of Antarctica (Figure 7(b)). The PREMA (FOZO) signature is also found in the Tasman Sea and the Ross Sea (e.g., Lanyon, 1994; Finn *et al*., 2005; Aviado *et al*., 2015). The LSVP also extends to the South Pacific ocean islands at depth of 500–600 km. Meanwhile, the upper mantle LSVP on the western side of the AAR appears to separate from the AAR (KR1–2)–PAR LSVP by the AAD (or Zone A) region and also is connected through the SEIR LSVs to the western LSVs that extend from the Central Indian Ridge (see Courtillot *et al*. 2003; Montelli *et al*. 2006; Ritsema *et al*. 2011). This aspect is consistent with studies that suggest that the Pacific and Indian-types of upper mantle domains can be separated compositionally near the AAD–Zone A (e.g. Christie *et al*. 1998; Kempton *et al*. 2002; Hanan *et al*. 2004). Park *et al*. (2019) proposed the regional area that covers the AAR–westernmost PAR–New Zealand–East Australia–West Antarctica (including Ross Sea province) and exhibits similar Sr–Nd–Pb–Hf isotopic signatures, to be the Zealandia–Antarctic mantle province. The isotopic results of this study also show that the KR1 ST and the surrounding areas could belong to the Zealandia–Antarctic mantle province proposed by Park *et al*. (2019). However, the hypothesis of Park *et al*. (2019) is a comprehensive interpretation that includes not only the oceanic mantle domains but also continental Zealandia and Antarctica. In view of the development of the MOR system and related ocean islands, the KR1 ST and the surrounding MOR regions are more relevant in terms of adding fertile materials (i.e. ancient, recycled oceanic crust) to the PAR upper mantle component.

In the $^{208}Pb/^{204}Pb$ and $^{207}Pb/^{204}Pb$ *versus* $^{206}Pb/^{204}Pb$ plots, the KR1–2 MORs, KR1 ST and Balleny province basalts exhibit a mixing trend of a PAR-type DMM and South Pacific Cook–Austral chain basalts (Figure 4). Hanan *et al*. (2004) noted that the Pacific upper mantle composition could be explained by processes related to seafloor subduction, whereas the Indian upper mantle composition could be affected by detachment and dispersal of lower continental crust related to the break-up of Gondwana and

that their distinction is bounded by the AAD region. The South Pacific is an area less affected by the break-up of Gondwana. Among them, the ocean islands and seamounts in the Cook–Austral chain retain their PREMA (FOZO)–HIMU-dominant components (Chauvel et al., 1997; Bonneville *et al*., 2002, 2006; Stracke *et al*., 2005; Stracke, 2012). In addition, it has been noted that the PREMA (FOZO)–HIMU components develop under the influence of ancient, recycled oceanic crust (Hanan and Graham, 1996; Stracke *et al*. 2005; Timm *et al*., 2011; Stracke 2012; Castillo, 2015; Homrighausen *et al*. 2018).

Although it is difficult to define the regional geologic processes in the Pacific and Indian Oceans from the limited isotopic data obtained from the KR1 region, it is important to point out that the upper mantle beneath the KR1 region may retain mixing components between the Pacific-type DMM and the ancient oceanic lithosphere (especially the oceanic crust) and that the KR1 ST alkaline basalts generally represent the enriched composition of the upper mantle beneath the KR1 region. In the Cook–Austral chain, the Rurutu young–Mauke–Atiu volcanoes, characterized by the most radiogenic Pb in the Rurutu young lava, exhibit a PREMA (FOZO) isotopic signature showing similar to that of the KR1 ST–Balleny province alkaline basalts in the $^{208}Pb/^{204}Pb$ and $^{207}Pb/^{204}Pb$ *versus* $^{206}Pb/^{204}Pb$ isotope plots (Figure 4). The PREMA (FOZO) signatures of the Rurutu young–Mauke–Atiu basalts have been interpreted as the results of melting of recycled, ancient oceanic lithosphere entrained by mantle plume (Dupuy *et al*., 1989; McNutt *et al*., 1997; Stracke *et al*. 2005; Stracke 2012). The enrichment direction of the KR1 ST–Balleny alkaline basalts to the Rurutu young basalts from the South Pacific Ocean in the Pb isotope spaces indicates that the mantle domains beneath these two regions (the KR1 ST-Balleny and the Rurutu) have undergone similar geologic processes in terms of the recycling of enriched crust, rather than a direct connection of the Rurutu mantle plume from the South Pacific Superswell to the study area. We presume that the KR1 segment, including the Balleny province, may have experienced a mantle plume event that resembled the Rurutu region after/during the break-up of Gondwana. The upper mantle domain of the KR1 and the adjacent region may have been altered by this kind of mantle plume event and had lithological composition to that of a DMM + fertile blobs (e.g. recycled, ancient oceanic crust) during the Cenozoic. We presume that the coexistence of the alkaline basalts and enriched tholeiites in the KR1 ST may reflect volcanic events related to sub-MOR mantle convection, which generally occurs at the peripheries of the MOR (e.g. Niu and Batiza 1997; Niu *et al*. 2002; Anderson 2006; Beutel and Anderson 2007; Ballmer *et al*., 2013). Alternatively, the topographic highs of the ridge crests near the KR1 ST and the Southwestern seamount province and their enriched MORB isotopic ratios (shown in Figure 6) suggest the possibility that a small- to medium-size mantle upwelling that originated from the lower mantle could now govern the KR1 ST, the Southwestern seamount province and the adjacent areas and that these seamounts and seamount chain represent short-lived hotspot volcanoes produced by ridge–hotspot interactions. Therefore, to answer the questions regarding whether the KR1 ST is the product of i) volcanic activity caused by shallow rifting or ii) small-size deep mantle upwelling from the lower mantle, a precise study of the seismic tomography of the KR1 segment and the surrounding region should be conducted in the future.

## 7. Conclusions

(1) The KR1 ST is a volcanic seamount chain located at the eastern end of the AAR that has developed parallel to the KR1 southeast spreading direction. The KR1 ST is ~60 km long, has a maximum height ~1600 m and consists of alkaline basalts and tholeiites. The (U–Th)/He and K–Ar ages of the basalts range from 0.4 Ma to ≤1.3 Ma, indicating that their ages are mostly younger than the surrounding seafloor ages, estimated using linear magnetic anomalies.

(2) Alkaline basalts from the KR1 ST exhibit PREMA (FOZO) compositions with respect to Sr, Nd and Pb isotopic ratios ($^{87}Sr/^{86}Sr$ = 0.7030–0.7033; $^{143}Nd/^{144}Nd$ = 0.5128–0.5130; $^{206}Pb/^{204}Pb$ = 19.52–19.91), which are similar to those of the Balleny province located ~450 km southeast of the KR1 ST along its spreading direction.

(3) Tholeiites from the KR1 ST exhibit intermediate isotopic compositions ($^{87}Sr/^{86}Sr$ = 0.7028–0.7029; $^{143}Nd/^{144}Nd$ = ~0.5130; $^{206}Pb/^{204}Pb$ = 18.89–18.93; $^{3}He/^{4}He$ = 7.63 ± 0.13 (R/RA)) between PREMA (FOZO) and DMM, overlapping the isotopic range of the KR1 MORB, and exhibit compositional similarities to E-MORB.

(4) Possible magma sources of the alkaline basalts are inferred to be recycled oceanic crust (i.e. eclogite) that underwent ancient subduction processes, with sub-KR1 DMM. Whereas, the main source materials of the tholeiitic magmas are presumed to be DMM-dominant lithology with minor eclogite portions.

(5) The KR1 ST is a composite hotspot chain consisting of various alkalic and tholeiitic materials. They are likely the products of upper mantle upwelling and spreading that delivered various amounts of fertile blobs of recycled oceanic crust to the sub-KR1 region.

## Acknowledgments

We are grateful to the captain and crews of the R/VIB *Araon* for their assistance during the cruise and thank In-Sung Yoo and Pil-Mo Kang for analytical supports and Seung-Ah Ha for isotope chemical separation. We thank Jung-Jin Moon for assistance with the electron microprobe analyses supported the early results of this study. We also thank chief editor Robert J. Stern for his guidance. Jörg Geldmacher and an anonymous reviewer are appreciated for constructive comments and suggestions which have improved greatly the manuscript.

## Disclosure statement

No potential conflict of interest was reported by the authors.

## Funding

This study was supported by the Korea Polar Research Institute (KOPRI) under Grant [PE20200].

## ORCID

Sang-Bong Yi http://orcid.org/0000-0001-6253-5420
Hirochika Sumino http://orcid.org/0000-0002-4689-6231

## References

Albarède, F., Luais, B., Fitton, G., Semet, M., Kaminski, E., Upton, B. G.J., Bachèlery, P., and Cheminée, J.-L., 1997, The geochemical regimes of Piton de la Fournaise Volcano (Réunion) during the last 530 000 years: Journal of Petrology, v. 38, no. 2, p. 171–201. doi10.1093/petroj/38.2.171.

Albarède, F., and van der Hilst, R.D., 1999, New mantle convection model may reconcile conflicting evidence: Eos, Transactions American Geophysical Union, v. 80, no. 45, p. 535–539. doi10.1029/EO080i045p00535.

Amma-Miyasaka, M., and Nakagawa, M., 2002, Origin of anorthite and olivine megacrysts in island-arc tholeiites: petrological study of 1940 and 1962 ejecta from Miyake-jima volcano, Izu-Mariana arc: Journal of Volcanology and Geothermal Research, v. 117, p. 263-283.

Anderson, D.L., 1998, The scales of mantle convection: Tectonophysics, v. 284, no. 1–2, p. 1–17. doi10.1016/S0040-1951(97)00169-8.

Anderson, D.L., 2000, The thermal state of the upper mantle; no role for mantle plumes: Geophysical Research Letters, v. 27, no. 22, p. 3623–3626. doi10.1029/2000GL011533.

Anderson, D.L., 2006, Speculations on the nature and cause of mantle heterogeneity: Tectonophysics, v. 416, no. 1–4, p. 7–22. doi10.1016/j.tecto.2005.07.011.

Aviado, K.B., Rilling-Hall, S., Bryce, J.G., and Mukasa, S.B., 2015, Submarine and subaerial lavas in the West Antarctic Rift System : Temporal record of shifting magma source components from the lithosphere and asthenosphere: Geochemistry Geophysics Geosystems, v. 16, p. 4344-4361, doi: 10.1002/2015GC006076

Ballmer, M.D., Conrad, C.P., Smith, E.I., and Harmon, N., 2013, Non-hotspot volcano chains produced by migration of shear-driven upwelling toward the East Pacific Rise: Geology, v. 41, no. 4, p. 479–482. doi10.1130/G33804.1.

Beutel, E., and Anderson, D.L., 2007, Ridge-crossing seamount chains: A nonthermal approach, *in* Foulger, G.R., and Jurdy, D.M., eds., Plates, plumes and planetary processes: Geological Society of America Special Paper Vol. 430: Boulder, Colorado: Geological Society of America, p. 375–386. doi:10.1130/2007.2430(19).

Bonneville, A., Dosso, L., and Hildenbrand, A., 2006, Temporal evolution and geochemical variability of the South Pacific superplume activity: Earth and Planetary Science Letters, v. 244, p. 251-269

Bonneville, A., Le Suavé, R., Audin, L., Clouard, V., Dosso, L., Gillot, P.Y., Janney, P., Jordhl, K., and Maamaatuaiahutapu, K., 2002. Arago seamount: the missing hotspot found in the Austral Islands: Geology, v. 30, p. 99-119.

Borisova, A.Y., Belyatsky, B.V., Portnyagin, M.V., and Sushchevskaya, N.M., 2001, Petrogenesis of an olivine-phyric basalts from the Aphanasey Nikitin Rise: evidence for contamination by cratonic lower continental crust: Journal of Petrology, v. 42, p. 277-319.

Cande, S.C., and Stock, J.M., 2004, Pacific-Antarctic-Australia motion and the formation of the Macquarie Plate: Geophysical Journal International, v. 157, no. 1, p. 399–414. doi10.1111/j.1365-246X.2004.02224.x.

Castillo, P., 2015, The recycling of marine carbonates and sources of HIMU and FOZO ocean island basalts: Lithos, v. 216-217, p. 254-263.

Chadwick, J., Keller, R., Kamenov, G., Yogodzinski, G., and Luptop, J., 2014, The Cobb hot spot: HIMU-DMM mixing and melting controlled by a progressively thinning lithospheric lid: Geochemistry Geophysics Geosystems, v. 15, p. 3107-3122, doi: 10.1002/2014GC005334

Chauvel, C., McDonough, W., Guille, G., Maury, R., and Duncan, R., 1997, Contrasting old and young volcanism in Rurutu Island, Austral chain: Chemical Geology, v. 139, no. 1–4, p. 125–143. doi10.1016/S0009-2541(97)00029-6.

Chen, J.H., Edwards, R.L., and Wasserburg, G.J., 1986, $^{238}$U, $^{234}$U and $^{232}$Th in seawater: Earth and Planetary Science Letters, v. 80, no. 3–4, p. 241–251. doi10.1016/0012-821X(86)90108-1.

Choi, H., Kim, -S.-S., Dyment, J., Granot, R., Park, S.-H., and Hong, J.K., 2017, The kinematic evolution of the Macquarie Plate: a case study for the fragmentation of oceanic lithosphere: Earth and Planetary Science Letters, v. 478, p. 132–142. doi:10.1016/j.epsl.2017.08.035.

Christie, D.M., Pedersen, R.-B., Miller, J., and Baldauf, J., 1999, Australian–Antarctic discordance: Mantle reservoirs and migration associated with Australian-Antarctic rifting: Ocean drilling program, LEG187 scientific prospectus: College Station, TX: Texas A&M University, p. 72 p.

Christie, D.M., West, B.P., Pyle, D.G., and Hanan, B.B., 1998, Chaotic topography, mantle flow and mantle migration in the Australian–Antarctic discordance: Nature, v. 394, no. 6694, p. 637–644. doi10.1038/29226.

Clague, D.A., and Sherrod, D.R., 2014, Growth and degradation of Hawaiian volcanoes, *in* Poland, M.P., Takahashi, T.J., and Landowski, C.M., eds., Characteristics of Hawaiian volcanoes:

U.S. Geological Survey Professional Paper 1801, U.S. Geological Survey, Reston, Virginia, p. 97–146.

Clouard, V., and Bonneville, A., 2001, How many Pacific hotspots are fed by deep-mantle plumes?: Geology, v. 29, no. 8, p. 695–698. doi10.1130/0091-7613(2001)029<0695:HMPHAF>2.0.CO;2.

Cordery, M.J., Davies, G.F., and Campbell, I.H., 1997, Genesis of flood basalts from eclogite-bearing mantle plumes: Journal of Geophysical Research, v. 102, no. B9, p. 20179–20197. doi10.1029/97JB00648.

Courtillot, V., Davaille, A., Besse, J., and Stock, J., 2003, Three distinct types of hotspots in the Earth's mantle: Earth and Planetary Science Letters, v. 205, no. 3–4, p. 295–308. doi10.1016/S0012-821X(02)01048-8.

Cousens, B.L., 1996, Depleted and enriched upper mantle sources for basaltic rocks from diverse tectonic environments in the northeast Pacific Ocean: the generation of ocean alkaline vs. tholeiitic basalts, Basu, A.R., and Hart, S. R., eds., Earth processes: Reading the isotopic code: Geophysical Monography, v. 95, p.207-231, American Geophysical Union.

Dalrymple, G.B., Moore, J.G., 1968, Argon-40: Excess in submarine pillow basalts from Kilauea volcano, Hawaii: Science, v. 161, p. 1132–1135.

Dalrymple, G.B., 1969, $^{40}Ar/^{36}Ar$ analyses of historic lava flows: Earth and Planetary Science Letter, v. 6, p. 47–55.

Dasgupta, R., Hirschmann, M.M., and Stalker, K., 2006, Immiscible transition from carbonate-rich to silicate-rich melts in the 3 GPa melting interval of eclogite + $CO_2$ and genesis of silica-undersaturated ocean island lavas: Journal of Petrology, v. 47, no. 4, p. 647–671. doi10.1093/petrology/egi088.

Dasgupta, R., Hirschmann, M.M., and Smith, N.D., 2007, Partial melting experiments of peridotite + $CO_2$ at 3 GPa and genesis of alkalic ocean island basalts: Journal of Petrology, v. 48, 2093-2124

Davies, F.A., Hirschmann, M.M., and Humayun, M., 2011, The composition of the incipient partial melt of garnet peridotite at 3 GPa and the origin of OIB. Earth and Planetary Science Letter, v. 308, p. 380-390.

Davies, G.F., 1990, Mantle plumes, mantle stirring and hotspot chemistry: Earth and Planetary Science Letters, v. 99, no. 1–2, p. 94–109. doi10.1016/0012-821X(90)90073-7.

Dilek, Y., and Thy, P., 2009, Island arc tholeiites to boninitic melt evolution of the the Cretaceous Kizildag (Turkey) ophiolite: model for multi-stage early arc-forearc magmatism in Tethyan subduction factories: Lithos, v. 113, p. 68-87.

Dostal, J., and MacRae, A., 2018, Cretaceous basalts of the High Arctic large igneous province at Axel Heiberg Island (Canada): Volcanic stratigraphy, geodynamic setting and origin: Geological Journal, doi: 10.1002/gj.3132

Doucet, S., Weis, D., Scoates, J.S., Debaille, V., and Giret, A., 2004, Geochemical and Hf–Pb–Sr–Nd isotopic constraints on the origin of the Amsterdam–St. Paul (Indian Ocean) hotspot basalts: Earth and Planetary Science Letters, v. 218, no. 1–2, p. 179–195. doi10.1016/S0012-821X(03)00636-8.

Dupré, B., and Allègre, C.J., 1983, Pb–Sr isotope variation in Indian Ocean basalts and mixing phenomena: Nature, v. 303, no. 5913, p. 142–146. doi10.1038/303142a0.

Dupuy, C., Barsczus, H.G., Dostal, J., Vidal, P., and Liotard, J.-M., 1989, Subduction and recycled lithosphere as the mantle source of oceanic island basalts from southern Polynesia, central Pacific: Chemical Geology, v. 77, p. 1-18.

Dyment, J., Lin, J., and Baker, E.T., 2007, Ridge-hotspot interactions: what mid-ocean ridges tell us about deep Earth processes: Oceanography, v. 20, no. 1, p. 102–115. doi10.5670/oceanog.2007.84.

Edwards, C.M.H., Menzies, M.A., Thirwall, M.F., Morris, J.D., Leeman, W.P., and Harmon, R.S., 1994, The transition to potassic alkaline volcanism in island arcs: the Ringgit-Beser Complex, East Java, Indonesia: Journal of Petrology, v. 35, p. 1557-1595.

Eggler, D.H., 1974, Effect of $CO_2$ on the melting of peridotite: Carnegie Institution Of Washington Yearbook, v. 74, p. 215-224.

Embleton, B.J.J., 1984, Magnetic properties of oriented rock samples from Sturge Island and Sabrina Island in the Balleny Group, Lewis, E., eds., Voyage to the ice, The Antarctic expedition of Solo: p. 128-131, Australian Broadcasting Commission, Sydney

Farley, K.A., Kohn, B.P., and Pillan, B., 2002, The effects of secular disequilibrium on (U–Th)/He systematics and dating of Quaternary volcanic zircon and apatite: Earth and Planetary Science Letters, v. 201, no. 1, p. 117–125. doi10.1016/S0012-821X(02)00659-3.

Farley, K.A., Natland, J.H., and Craig, H., 1992, Binary mixing of enriched and undegassed (primitive?) mantle components (He, Sr, Nd, Pb) in Samoan Lavas: Earth and Planetary Science Letters, v. 111, p. 183-199.

Finn, C.A., Müller, R.D., and Panter, K.S., 2005, A Cenozoic diffuse alkaline magmatic province (DAMP) in the southwest Pacific without rift or plume origin. Geochemistry Geophysics Geosystems, v. 6, Q02005, doi: 10.1029/2004GC000723

Fisher, D.E., 1972, U/He ages as indicators of excess argon in deep sea basalts: Earth and Planetary Science Letters, v. 14, no. 2, p. 225–258. doi10.1016/0012-821X(72)90016-7.

Fisher, 1981. Quantitative retention of magmatic argon in a glassy basalt: Nature, v. 290, p. 42–43.

Fitton, J.G., 2007, The OIB paradox, *in* Foulger, G.R., and Jurdy, D.M., eds., Plates, plumes and planetary processes: Geological Society of America Special Paper 430, Geological Society of America, Boulder, Colorado, p. 387-412. doi:10.1130/2007.2430(20).

Fornari, D.J., Perfit, M.R., Allan, J.F., Batiza, R., Haymon, R., Barone, A., Ryan, W.B.F., Smith, T., Simkin, T., and Luckman, M.A., 1988, Geochemical and structural studies of the Lamont seamounts: seamount as indicators of mantle process: Earth and Planetary Science Letters, v. 89, p. 63-83.

Füri, E., Hilton, D.R., Murton, B.J., Hémond, C., Dyment, J., and Day, J.M.D., 2011, Helium isotope variations between Réunion Island and the Central Indian Ridge (17°–21°S): New evidence for ridge–hot spot interaction: Journal of Geophysical Research, v. 116, no. B2, p. B02207. doi:10.1029/2010JB007609.

Gale, A., Dalton, C.A., Langmuir, C.H., Su, Y., and Schilling, J.-G., 2013, The mean composition of ocean ridge basalts: Geochemistry, Geophysics, Geosystems, v. 14, no. 3, p. 489–518. doi:10.1029/2012GC004334.

Garcia, M.O., 2015, How and why Hawaiian volcanism has become pivotal to our understanding of volcanoes from their source to the surface, *in* Carey, R., Cayol, V., Poland, M., and Weis, D., eds., Hawaiian volcanoes: from source to surface: Geophysical Monograph, volume 208: American Geophysical Union, John Wiley & Sons, Hoboken, New Jersey, p. 1–18.

Geldmarcher, J., Hoernle, K., van den Bogaard, P., Zankl, G., and Garbe-Schönberg, D., 2001, Earlier history of the ≥ 70-Ma-old Canary hotspot based on the temporal and geochemical evolution of the Selvagen Archipelago and neighboring seamounts in the eastern north atlantic: Journal of Volcanology and Geothermal Research, v. 111, p. 55-87.

Geldmarcher, J., Hoernle, K., van den Bogaard, P., Duggen, S., and Werner, R., 2005, New $^{40}Ar/^{39}Ar$ age and geochemical data from seamounts in the Canary and Madeira volcanic provinces: Support for the mantle plume hypothesis: Earth and Planetary Science Letters, v. 237, p. 85-101.

Geldmarcher, J., Hoernle, K., Klügel, A., van den Bogaard, P., and Duggen, S., 2006, A geochemical transect across a heterogeneous mantle upwelling: implications for the evolution of the madeira hotspot in space and time: Lithos, v. 90, p. 131-144

Graham, D.W., 2002, Noble gas isotope geochemistry of mid-ocean ridge and ocean island basalts: characterization of mantle source reservoirs: Reviews in Mineralogy and Geochemistry, v. 47, p. 247-317.

Green, T.H., 1992, Petrology and geochemistry of basaltic rocks from the Balleny Islands, Antarctica: Australian Journal of Earth Sciences, v. 39, 603-617

Hanan, B.B., Blichert-Toft, J., Pyle, D.G., and Christie, D.M., 2004, Contrasting origins of the upper mantle revealed by hafnium and lead isotopes from the Southeast Indian Ridge: Nature, v. 432, no. 7013, p. 91–94. doi10.1038/nature03026.

Hanan, B.B., and Graham, D.W., 1996, Lead and helium isotope evidence from oceanic basalts for a common deep source of mantle plumes: Science, v. 272, p. 991-995

Hanyu, T., 2014, Deep plume origin of the louisville hotspot: noble gas evidence: Geochemistry Geophysics Geosystems, v. 15, p. 565-576, doi: 10.1002/2013GC005085

Hart, S.R., 1984, A large-scale isotope anomaly in the Southern Hemisphere mantle: Nature, v. 309, no. 5971, p. 753–757. doi10.1038/309753a0.

Hart, S.R., Hauri, E.H., Oschmann, L.A., and Whitehead, J.A., 1992, Mantle plumes and entrainment: isotopic evidence: Science, v. 256, no. 5056, p. 517–520. doi10.1126/science.256.5056.517.

Hauri, E.H., 1996, Major-element variability in the Hawaiian mantle plume: Nature, v. 382, no. 6590, p. 415–419. doi10.1038/382415a0.

Herzberg, C., 2006, Petrology and thermal structure of the hawaiian plume form Mauna Kea volcano: Nature, v. 444, 605-609.

Hilton, D.R., and Porcelli, 2003, Noble gases as mantle tracers, Carlson, R.W., eds., Treatise on Geochemistry, Vol. 2: The mantle and core: Elsevier, Oxford, p. 277–318

Hilton, D.R., Gronvold, K., Macpherson, C.G., and Castillo, P.R., 1999, Extreme $^{3}He/^{4}He$ ratios in northwest Iceland: constraining the common component in mantle plume: Earth and Planetary Science Letters, v. 173, p. 53-60.

Hirano, N., Takahashi, E., Yamamoto, J., Abe, N., Ingle, S.P., Kaneoka, I., Hirata, T., Kimura, J.-I., Ishii, T., Ogawa, Y., Machida, S., and Suyehiro, K., 2006, Volcanism in response to plate flexure: Science, v. 313, no. 5792, p. 1426–1428. doi10.1126/science.1128235.

Hirose, K., 1997, Partial melting compositions of carbonated peridotite at 3 GPa and role of $CO_2$ in alkali-basalt magma generation: Geophysical Research Letters, v. 24, p. 2837–2840

Hirose, K., and Kusiro, I., 1993, Partial melting of dry peridotites at high pressures: determination of compositions of melts segregated from peridotite using aggregates of diamond: Earth and Planetary Science Letters, v. 114, p. 477–489

Hirschmann, M.M., Kogiso, T., Baker, M.B., and Stolper, E.M., 2003, Alkalic magmas generated by partial melting of garnet pyroxenite: Geology, v. 31, no. 6, p. 481–484. doi10.1130/0091-7613(2003)031<0481:AMGBPM>2.0.CO;2.

Hoernle, K., and Schmincke, H.-U., 1993, The petrology of the tholeiites through melilite nephelinites on Gran Canaria, Canary Islands: Crystal fractionation, accumulation, and depths of melting: Journal of Petrology, v. 34, no. 3, p. 573–597. doi10.1093/petrology/34.3.573.

Homrighausen, S., Hoernle, K., Hauff, F., Geldmacher, J., Wartho, J.-A., van den Bogaard, P., and Garbe-Schönberg, D., 2018, Global distribution of the HIMU end member: Formation through Archean plume-lid tectonics: Earth-Science Reviews, v. 182, p. 85–101. doi:10.1016/j.earscirev.2018.04.009.

Hoernle, K., Hauff, F., Werner, R., van den Boggard, P., Gibbson, A.D., Conrad, S., and Müller, R.D., 2011a, Origin of Indian Ocean Seamount Province by shallow recycling of continental lithosphere: Nature Geoscience, v. 4, p. 883–887.

Hoernle, K., Hauff, F., Kokfelt, T.F., Haase, K., Garbe-Schönberg, D., and Werner, R., 2011b, On- and off-axis chemical heterogeneities along the South Atlantic Mid-Ocean-Ridge (5-11° S): Shallow or deep recycling of ocean crust and/or intraplate volcanism?: Earth and Planetary Science Letters, v. 306, p. 86–97.

Hofmann, A.W., 2003, Sampling mantle heterogeneity through ocean basalts: Isotopes and trace elements, Carlson, R.W., eds., Treatise on Geochemistry, Vol. 2: The mantle and core: Elsevier, Oxford, p. 61–101.

Humphreys, E.R., and Niu, Y., 2009, On the composition of ocean island basalts (OIB): the effects of lithospheric thickness variation and mantle metasomatism: Lithos, v. 112, p. 118-136

Ishizuka, O., Tani, K., Reagan, M.K., Kanayama, K., Umino, S., Harigane, Y., Sakamoto, I., Miyajima, Y., Yuasa, M., and Dunkley, D.J., 2011, The timescales of subduction initiation and subsequent evolution of an oceanic island arc: Earth and Planetary Science Letters, v. 306, p. 229–240

Janney, P.E., Macdougall, J.D., Natland, J.H., and Lynch, M.A., 2000, Geochemical evidence from the Pukapuka volcanic ridge system for a shallow enriched mantle domain beneath the South Pacific Superswell: Earth and Planetary Science Letters, v. 181, p. 47–60

Jackson, M.G., Becker, T.W., and Konter, J.G., 2018, Evidence for a deep mantle source for EM and HIMU domains from integrated geochemical and geophysical constraints: Earth and Planetary Science Letters, v. 484, p. 154–167. doi:10.1016/j.epsl.2017.11.052.

Jambon, A., and Shelby, J.S., 1980, Helium diffusion and solubility in obsidians and basaltic glass in the range 200–300°C: Earth and Planetary Science Letters, v. 51, no. 1, p. 206–218. doi10.1016/0012-821X(80)90268-X.

Jenkins, C.J., Packham, G.H., Hubble, T.C., Quilty, P.G., and Adams, C.J., 1992, Trace of the Balleny hotspot in the Tasman Sea and Southern Ocean from 70 Ma to present: First Australian Marine Geoscience Meeting, Canberra.

Johnson, G.L., Kyle, P.R., Vanney, J.R., and Campsie, J., 1982, Geology of Scott and Balleny Islands, Ross Sea, Antarctica, and morphology of adjacent seafloor: New Zealand Journal

of Geology and Geophysics, v. 25, no. 4, p. 427–436. doi10.1080/00288306.1982.10421508.

Kellogg, L.H., Hager, B.H., and van der Hilst, R.D.,1999, Compositional stratification in the deep mantle: Science, v. 283, no. 5409, p. 1881–1884. doi10.1126/science.283.5409.1881.

Kempton, P.D., Pearce, J.A., Barry, T.L., Fitton, J.G., Langmuir, C., and Christie, D.M., 2002, Sr-Nd-Pb-Hf isotope results from ODP leg 187: Evidence for Mantle dynamics of the Australian-Antarctic discordance and origin of the Indian MORB source: Geochemistry, Geophysics, Geosystems, v. 3, no. 12, p. 1074. doi:10.1029/2002GC000320.

Kennedy, A.K., Hart, S.R., and Frey, F.A., 1990, Composition and isotopic constraints on the petrogenesis of alkaline arc lavas: Lihir Island, Papua New Guinea: Journal of Geophysical Research, v. 95, p. 6929-6942.

Keshav, S., Gudfinnsson, G.H., Sen, G., and Fei, Y., 2004, High-pressure melting experiments on garnet clinopyroxenite and the alkalic to tholeiitic transition in ocean-island basalts: Earth and Planetary Science Letters, v. 223, p. 365-379

Kipf, A., Hauff, F., Werner, R., Gohl, K., van den Bogaard, P., Hoernle, K., Maicher, D., Klügel, A., 2014, Seamounts off the West Antarctic margin: A case for non-hotspot driven intraplate volcanism: Gondwana Research, v. 25, p. 1660–1679.

Kim, J., Pak, S.-J., Moon, J.-W., Lee, S.-M., Oh, J., and Stuart, F.M., 2017, Mantle heterogeneity in the source region of mid-ocean ridge basalts along the northern Central Indian Ridge (8°S–17°S): Geochemistry Geophysics Geosystems, v. 18, doi:10.1002/2016GC006673

Kim, J., Park, J.-W., Lee, M.J., Lee, J.I., and Kyle, P.R., 2019, Evolution of alkalic magma systems: Insight from coeval evolution of sodic and potassic fractionaltion lineages at the Pleiades Volcanic Complex, Antarctica: Journal of Petrology, v. 60, p. 117-150

Kinzler, R.J., and Grove, T.L., 1993, Corrections and further discussion of the primary magmas of mid-ocean ridge basalts, 1 and 2: Journal of Geophysical Research, v. 98, p. 22339-22347.

Kogiso, T., 2004, High-pressure partial melting of mafic lithologies in the mantle: Journal of Petrology, v. 45, no. 12, p. 2407–2422. doi10.1093/petrology/egh057.

Kogiso, T., Hirose, K., and Takahashi, E., 1998, Melting experiments on homogeneous mixtures of peridotite and basalt: application to the genesis of ocean island basalts: Earth and Planetary Science Letters, v. 162, no. 1–4, p. 45–61. doi10.1016/S0012-821X(98)00156-3.

Kogiso, T., Hirschmann, M.M., and Frost, D.J., 2003, High-pressure partial melting of garnet pyroxenite: possible mafic lithologies in the source of ocean island basalts: Earth and Planetary Science Letters, v. 216, no. 4, p. 603–617. doi10.1016/S0012-821X(03)00538-7.

Koppers, A.A.P., 2011, Mantle plumes persevere: Nature Geoscience, v. 4, no. 12, p. 816–817. doi10.1038/ngeo1334.

Kushiro, I., 1996, Partial melting of a fertile mantle peridotite at high pressures: An experimental study using aggregates of diamond, in Basu, A. and Hart, S.R., eds., Earth processes: Reading the isotopic code: Geophygical Monograph 95, American Geophysical Union, Washington, DC, p. 109–122.

Kushiro, I., 2001, Partial melting experiments on peridotite and origin of mid-ocean ridge basalts: Annual Review of Earth and Planetary Sciences, v. 29, p. 71–107.

Lanyon, R., 1994, Mantle reservoirs and mafic magmatism associated with the break-up of Gondwana–the Balleny plume and the Australian-Antarctic discordance. U-Pb zircon dating of a Proterozoic mafic dyke swarm in the Vestfold Hills, East Antarctica [Ph.D. thesis]: Hobart, Tasmania, University of Tasmania, 402 p.

Lanyon, R., Varne, R., and Crawford, A.J., 1993, Tasmanian Tertiary basalts, the Balleny plume, and opening of the Tasman Sea (southwest Pacific Ocean): Geology, v. 21, no. 6, p. 555–558. doi10.1130/0091-7613(1993)021<0555:TTBTBP>2.3.CO;2.

Lee, M.J., Lee, J.I., Kim, T.H., Lee, J., and Nagao, K., 2015, Age, geochemistry and Sr-Nd-Pb isotopic compositions of alkali volcanic rocks from Mt. Melbourne and the western Ross Sea, Antarctica: Geosciences Journal, v. 19, no. 4, p. 681–695. doi10.1007/s12303-015-0061-y.

Long, X., Geldmacher, J., Hoernle, K., Hauff, F., Wartho, J.-A., Garbe-Schönberg, D., and Grevemeyer, I., 2019, Age and origin of Researcher Ridge and an explanation for the 14° N anomaly on the Mid-Atlantic Ridge by plum-ridge interaction: Lithos, v. 326-327, 540-555

Mallik, A., and Dasgupta, R., 2012, Reaction between MORB-eclogite derived melts and fertile peridotite and generation of ocean island basalts: Earth and Planetary Science Letters, v. 329-330, p. 97–108.

Mallik, A., and Dasgupta, R., 2013, Reactive infiltration of MORB-eclogite-derived carbonated silicate melt into fertile peridotite at 3 GPa and genesis of alkalic magmas: Journal of Petrology, v. 54, p. 2267–2300.

Mallik, A., and Dasgupta, R., 2014, Effect of variable $CO_2$ on eclogite-derived andesite and lherzolite reaction at 3 GPa-Implications for mantle source characteristics of alkalic ocean island basalts: Geochemistry Geophysics Geosystems, v. 15, 1533–1557, doi:10.1009/2014GC005251

Matsuda, J., Matsumoto, T., Sumino, H., Nagao, K., Yamamoto, J., Miura, Y.N., Kaneoka, I., Takahata, N., and Sano, Y., 2002, The $^3He/^4He$ ratio of the new internal He Standard of Japan (HESJ).: Geochemical Journal, v. 36, no. 2, p. 191–195. doi10.2343/geochemj.36.191.

McDonough, W., and Sun, -S.-S., 1995, The composition of the Earth: Chemical Geology, v. 120, no. 3–4, p. 223–253. doi10.1016/0009-2541(94)00140-4.

McNutt, M.K., 2006, Another nail in the plume coffin?: Science, v. 313, no. 5792, p. 1394–1395. doi10.1126/science.1131298.

McNutt, M.K., Caress, D.W., Reynold, J., Jordahl, K.A., and Duncan, R.A., 1997, Failure of plume theory to explain midplate volcanism in the southern Austral islands, Nature, v. 389, p. 479-482.

Mertz, D.F., Sharp, W.D., and Haase, K.M., 2004, Volcanism on the Eggvin Bank (Central Norwegian-Greenland Sea, latitude ~71°N): age, source, and relationship to the Iceland and putative Jan Mayen plumes: Journal of Geodynamics, v. 38, no. 1, p. 57–84. doi10.1016/j.jog.2004.03.003.

Montelli, R., Nolet, G., Dahlen, F.A., and Masters, G., 2006, A catalogue of deep mantle plumes: New results from finite-frequency tomography: Geochemistry, Geophysics, Geosystems, v. 7, no. 11. doi:10.1029/2006GC001248.

Morgan, W.J., 1971, Convection plumes in the lower mantle: Nature, v. 230, no. 5288, p. 42–43. doi10.1038/230042a0.

Morgan, W.J., 1978, Rodriguez, Darwin, Amsterdam, . . ., a second type of hotspot island: Journal of Geophysical Research, v. 83, no. B11, p. 5355–5360. doi10.1029/JB083iB11p05355.

Nagao, K., Ogata, A., Miura, Y.N., and Yamaguchi, K., 1996, Ar isotope analysis for K–Ar dating using two modified-VG5400 Mass Spectrometers-I: Isotope dilution method: Journal of

the Mass Spectrometry Society of Japan, v. 44, no. 1, p. 39–61. doi10.5702/massspec.44.39.

Niu, Y., 2004, Bulk-rock major and trace element compositions of abyssal peridotites: Implications for mantle melting, melt extraction and post-melting processes beneath mid-ocean ridges: Journal of Petrology, v. 45, no. 12, p. 2423–2458. doi10.1093/petrology/egh068.

Niu, Y., 2008, The origin of alkaline lavas: Science, v. 320, p. 883–884.

Niu, Y., and Batiza, R., 1997, Trace element evidence from seamounts for recycled oceanic crust in the Eastern Pacific mantle: Earth and Planetary Science Letters, v. 148, no. 3–4, p. 471–483. doi10.1016/S0012-821X(97)00048-4.

Niu, Y., Regelous, M., Wendt, I.J., Batiza, R., and O'Hara, M.J., 2002, Geochemistry of near-EPR seamounts: importance of source vs. process and the origin of enriched mantle component: Earth and Planetary Science Letters, v. 199, no. 3–4, p. 327–345. doi10.1016/S0012-821X(02)00591-5.

Ozima, M., and Podosek, F.A., 2002, Noble gas geochemistry: Cambridge, UK: Cambridge University Press, p. 286.

Ozima, M., Saito, K., and Honda, M., 1977, Sea water weathering effect on K–Ar age of submarine basalts: Geochimica et Cosmochimica Acta., v. 41, p. 453-461.

Park, S.-H., Langmuir, C.H., Sims, K.W.W., Blichert-Toft, J., Kim, -S.-S., Scott, S.R., Lin, J., Choi, H., Yang, Y.-S., and Michael, P.J., 2019, An isotopically distinct Zealandia–Antarctic mantle domain in the Southern Ocean: Nature Geoscience, v. 12, no. 3, p. 206–214. doi10.1038/s41561-018-0292-4.

Pertermann, M., and Hirschmann, M.M., 2003, Anhydrous partial melting experiments on MORB-like eclogite: phase relations, phase compositions and mineral-melt partitioning of major elements at 2–3 GPa: Journal of Petrology, v. 44, p. 2173-2201.

Pettke, T., Kodolanyi, J., and Kamber, B.S., 2018, From ocean to mantle: new evidence for U-cycling with implications for the HIMU source and the secular Pb isotope evolution of Earth's mantle: Lithos, v. 316-317, p. 66–76. doi:10.1016/j.lithos.2018.07.010.

Poland, M.P., 2015, "Points requiring elucidation" about Hawaiian volcanism, *in* Carey, R., Cayol, V., Poland, M., and Weis, D., eds., Hawaiian volcanoes: from source to surface: Geophysical Monograph, volume 208: American Geophysical Union, John Wiley & Sons, Hoboken, New Jersey, p. 533–562.

Regan, M.K., McClelland, W.C., Girard, G., Goff, K.R., Peate, D.W., Ohara, Y., and Stern, R.J., 2013, The geology of the southern Mariana fore-arc crust: implications for the scale of Eocene volcanism in the western Pacific: Earth and Planetary Science Letters, v. 380, p. 41-51

Ritsema, J., Deuss, A., van Heijst, H.J., and Woodhouse, J.H., 2011, S40RTS: a degree-40 shear-velocity model for the mantle from new Rayleigh wave dispersion, teleseismic traveltime and normal-mode splitting function measurements: Geophysical Journal International, v. 184, no. 3, p. 1223–1236. doi10.1111/j.1365-246X.2010.04884.x.

Saito, K., 1978, Classification and generation of terrestrial rare gases, *in* Alexander Jr., E.C., and Ozima, M., eds., Terrestrial rare gases: Japan Scientific Society Press, Springer, Amsterdam, p. 145–153.

Schouten, H., Dick, H.J.B., and Klitgord, K.D., 1987, Migration of mid-ocean-ridge volcanic segments: Nature, v. 326, p. 835-839

Seidemann, D.E., 1977, Effects of submarine alteration on K–Ar dating of deep-sea igneous rocks: Geological Society of America Bulletin, v. 88, p. 1660-1666

Shervais, J.W., 2001, Birth, death, and resurrection: The life cycle of suprasubduction zone ophiolites: Geochemistry Geophysics Geosystems, v. 2, 2000GC000080

Shibata, T., and Yoshikawa, M., 2004, Precise isotope determination of trace amounts of Nd in magnesium-rich samples: Journal of the Mass Spectrometry Society of Japan, v. 52, no. 6, p. 317–324. doi10.5702/massspec.52.317.

Silver, P.G., Carlson, R.W., and Olson, P., 1988, Deep slabs, geochemical heterogeneity, and the large-scale structure of mantle convection: Investigation of an enduring paradox: Annual Review of Earth and Planetary Sciences, v. 16, no. 1, p. 477–541. doi10.1146/annurev.ea.16.050188.002401.

Sleep, N.H., 1990, Hotspots and mantle plumes: some phenomenology: Journal of Geophysical Research, v. 95, no. B5, p. 3736–6715. doi10.1029/JB095iB05p06715.

Sleep, N.H., 2002, Local lithospheric relief associated with fracture zones and ponded plume material: Geochemistry, Geophysics, Geosystems, v. 3, no. 12, p. 1–17. doi:10.1029/2002GC000376.

Smith, A.D., 2005, The streaky-mantle alternative to mantle plumes and its bearing on bulk-earth geochemical evolution, Foulger, G.R., Natland, J.H., Presnall, D.C., and Anderson, D.L., eds., Plates, Plumes, and Paradigms: Geological Society of America Special Paper, v. 388, p. 303-325.

Sobolev, A.V., Hofmann, A.W., Kuzmin, D.V., Yaxley, G.M., Arndt, N.T., Chung, S.-L., Danyushevsky, Elliot, Frey, T., Garcia, F.A., Gurenko, M.O., Kamenetsky, A.A., Kerr, V.S., Krivolutskaya, A. C., Matvienkov, N.A., Nikogosian, V.V., Rocholl, I.K., Sigurdsson, A., and Sushchevskaya, I.A., N.M., and Teklay, M., 2007, The amount of recycled crust in sources of mantle-derived melts: Science, v. 316, p. 412-417

Sobolev, A.V., Hofmann, A.W., Sobolev, S.V., and Nikogosian, I. K., 2005, An olivine-free mantle source of Hawaiian shield basalts: Nature, v. 434, p. 590-597

Spandler, C., Yaxley, G., Green, D.H., and Rosenthal, A., 2008, Phase relations and melting of anhydrous k-bearing eclogite from 1200 to 1600 ºc and 3 to 5 GPa: Journal of Petrology, v. 49, p. 771-795

Staudigel, H., and Clague, D.A., 2010, The geological history of deep-sea volcanoes: Biosphere, hydrosphere, and lithosphere interactions: Oceanography, v. 23, no. 1, p. 56–71. doi10.5670/oceanog.2010.62.

Staudigel, H., Davies, G.R., Hart, S.R., Marchant, K.M., and Smith, B.M., 1995, Large scale isotopic Sr, Nd and O isotopic anatomy of altered oceanic crust: DSDP/ODP sites 417/418: Earth and Planetary Science Letters, v. 130, no. 1–4, p. 169–185. doi10.1016/0012-821X(94)00263-X.

Stracke, A., 2012, Earth's heterogeneous mantle: A product of convection-driven interaction between crust and mantle: Chemical Geology, v. 330-331, p. 274–299. doi:10.1016/j.chemgeo.2012.08.007.

Stracke, A., Hofmann, A.W., and Hart, S.R., 2005, FOZO, HIMU, and the rest of the mantle zoo: Geochemistry, Geophysics, Geosystems, v. 6, no. 5. doi:10.1029/2004GC000824.

Sumino, H., Nagao, K., and Notsu, K., 2001, Highly sensitive and precise measurement of helium isotopes using a mass spectrometer with double collector system: Journal of the Mass Spectrometry Society of Japan, v. 49, no. 2, p. 61–68. doi10.5702/massspec.49.61.

Sun, S.S., and McDonough, W.F., 1989, Chemical and isotopic systematic of oceanic basalt: implications for mantle composition and processes, in Saunders, A.D., and Norry, M.J., eds., Magmatism in the ocean basins: Geological Society Special Publication, no. 42, The Geological Society of London, London, p. 313–345

Sun, C.-H., and Stern, R.J., 2001, Genesis of Mariana shoshonites: contribution of the subduction component: Journal of Geophysical Research, v. 106, p. 589-608

Takahashi, E., 1986, Melting of a dry peridotite KLB-1 up to 14 GPa: implications on the origin of peridotitic upper mantle: Journal of Geophysical Research, v. 91, p. 9367–9382

Timm, C., Hoernle, K., Werner, R., Hauff, F., van den Bogaard, P., Michael, P., Coffin, M.F., and Koppers, A., 2011, Age and geochemistry of the oceanic Mahihiki Plateau, SW Pacific: New evidence for a plume origin: Earth and Planetary Science Letters, v. 304, p. 135–146

Vlastelic, I., Dosso, L., Guillou, H., Bougault, H., Geli, L., Etoubleau, J., and Joron, J.L., 1998, Geochemistry of the Hollister Ridge: relation with the Louisville hotspot and Pacific-Antarctic Ridge: Earth and Planetary Science Letters, v. 160, p. 777–793

Vlastélic, I., Dossom, L., Bougault, H., Aslanian, D., Géli, L., Etoubleau, J., Bohn, M., Joron, J.-L., and Bollinger, C., 2000, Chemical systematics of an intermediate spreading ridge: the Pacific-Antarctic Ridge between 56°S and 66°S: Journal of Geophysical Research, v. 105, no. B2, p. 2915–2936. doi10.1029/1999JB900234.

Walter, M.J., 1998, Melting of garnet peridotite and the origin of komatiite and depleted lithosphere: Journal of Petrology, v. 39, p. 29-60.

Weis, D., and Frey, F.A.,2002, Submarine basalts of the Northern Kerguelen Plateau: Interaction between the Kerguelen plume and the Southeast Indian Ridge revealed at ODP Site 1140: Journal of Petrology, v. 43, no. 7, p. 1287–1309. doi10.1093/petrology/43.7.1287.

Weis, D., Frey, F.A., Schlich, R., Schaming, M., Montigny, R., Damasceno, D., Mattielli, N., Nicolaysen, K.E., and Scoates, J.S., 2002, Trace of the Kerguelen mantle plume: Evidence from seamounts between the Kerguelen Archipelago and Heard Island, Indian Ocean: Geochemistry, Geophysics, Geosystems, v. 3, no. 6, p. 1–27. doi:10.1029/2001GC000251.

White, W.M., 2010, Oceanic island basalts and mantle plumes: the geochemical perspective: Annual Review of Earth and Planetary Sciences, v. 38, no. 1, p. 133–160. doi10.1146/annurev-earth-040809-152450.

Willbold, M., and Stracke, A., 2010, Formation of enriched mantle components by recycling of upper and lower continental crust: Chemical Geology, v. 276, p. 188–197.

Wright, A.C., and Kyle, P.R., 1990, Balleny Islands, LeMasurier, W. E., and Thomson, J.W., eds., Volcanoes of Antarctic plate and Southern Oceans: Antarctic Research Series, v. 48, 449-451, American Geophysical Union, Washington D.C.

Yi, S.-B., Lee, M.J., Park, S.-H., Han, S., Yang, Y.S., and Choi, H., 2019, Occurrence of ice-rafted erratics and the petrology of the KR1 seamount trail from the Australian–Antarctic Ridge: International Geology Review, v. 61, no. 12, p. 1429–1445. doi10.1080/00206814.2018.1514669.

Yi, S.-B., Oh, C.-W., Pak, S.J., Kim, J., and Moon, J.-W., 2014, Geochemistry and petrogenesis of mafic-ultramafic rocks from the Central Indian Ridge, latitude 8°–17° S: denudation of mantle harzburgites and gabbroic rocks and compositional variation of basalts: International Geology Review, v. 56, no. 14, p. 1691–1719. doi10.1080/00206814.2014.955539.

Zindler, A., and Hart, S.R., 1986, Chemical geodynamics: Annual Review of Earth and Planetary Sciences, v. 14, no. 1, p. 493–571. doi10.1146/annurev.ea.14.050186.002425.